PEARL Inc.
Web: http://www.pearl-hifi.com 86008, 2106 33 Ave. SW, Calgary, AB; CAN T2T 1Z6
E-mail: custserv@pearl-hifi.com Ph: +.1.403.244.4434 Fx: +.1.403.245.4456
Perkins Electro-Acoustic Research Lab, Inc. ❦ Engineering and Intuition Serving the Soul of Music

Please note that the links in the PEARL logotype above are "live" and can be used to direct your web browser to our site or to open an e-mail message window addressed to ourselves.

To view our item listings on eBay, click here.

To see the feedback we have left for our customers, click here.

Sec. 107. - Limitations on exclusive rights: Fair Use

Notwithstanding the provisions of sections 106 and 106A, the fair use of a copyrighted work, including such use by reproduction in copies or phono records or by any other means specified by that section, for purposes such as criticism, comment, news reporting, teaching (including multiple copies for classroom use), scholarship, or research, is not an infringement of copyright. In determining whether the use made of a work in any particular case is a fair use the factors to be considered shall include:

1 - the purpose and character of the use, including whether such use is of a commercial nature or is for nonprofit educational purposes;

2 - the nature of the copyrighted work;

3 - the amount and substantiality of the portion used in relation to the copyrighted work as a whole; and

4 - the effect of the use upon the potential market for or value of the copyrighted work.

The fact that a work is unpublished shall not itself bar a finding of fair use if such finding is made upon consideration of all the above factors

TECHNICAL REVIEW

Characteristics of the Vold-Kalman Order Tracking Filter

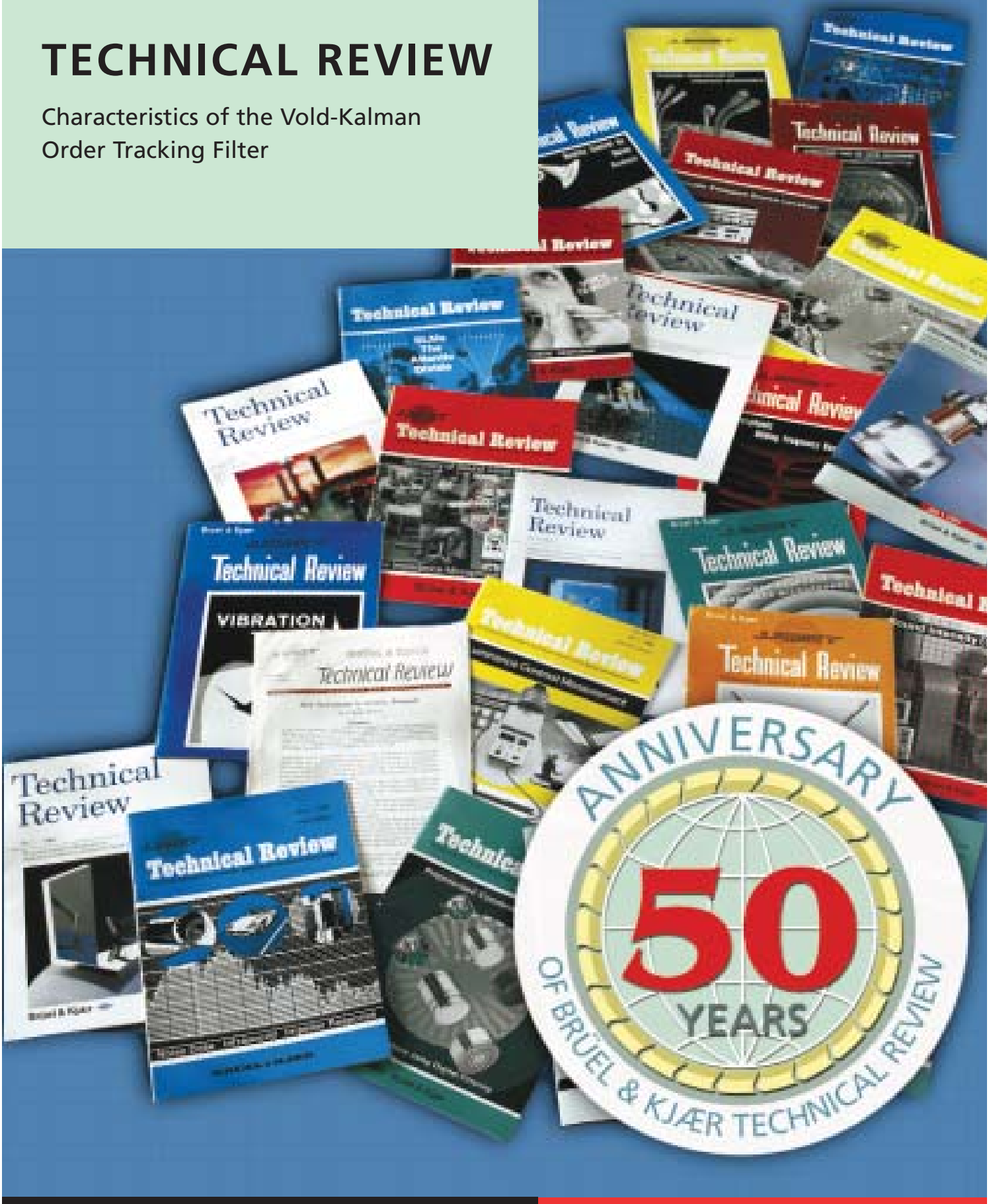

1999

Brüel & Kjær

Previously issued numbers of Brüel & Kjær Technical Review

1 – 1998 Danish Primary Laboratory of Acoustics (DPLA) as Part of the National Metrology Organisation
Pressure Reciprocity Calibration – Instrumentation, Results and Uncertainty
MP.EXE, a Calculation Program for Pressure Reciprocity Calibration of Microphones

1 – 1997 A New Design Principle for Triaxial Piezoelectric Accelerometers
A Simple QC Test for Knock Sensors
Torsional Operational Deflection Shapes (TODS) Measurements

2 – 1996 Non-stationary Signal Analysis using Wavelet Transform, Short-time Fourier Transform and Wigner-Ville Distribution

1 – 1996 Calibration Uncertainties & Distortion of Microphones.
Wide Band Intensity Probe. Accelerometer Mounted Resonance Test

2 – 1995 Order Tracking Analysis

1 – 1995 Use of Spatial Transformation of Sound Fields (STSF) Techniques in the Automative Industry

2 – 1994 The use of Impulse Response Function for Modal Parameter Estimation
Complex Modulus and Damping Measurements using Resonant and Non-resonant Methods (Damping Part II)

1 – 1994 Digital Filter Techniques vs. FFT Techniques for Damping Measurements (Damping Part I)

2 – 1990 Optical Filters and their Use with the Type 1302 & Type 1306 Photoacoustic Gas Monitors

1 – 1990 The Brüel & Kjær Photoacoustic Transducer System and its Physical Properties

2 – 1989 STSF — Practical Instrumentation and Application
Digital Filter Analysis: Real-time and Non Real-time Performance

1 – 1989 STSF — A Unique Technique for Scan Based Near-Field Acoustic Holography Without Restrictions on Coherence

2 – 1988 Quantifying Draught Risk

1 – 1988 Using Experimental Modal Analysis to Simulate Structural Dynamic Modifications
Use of Operational Deflection Shapes for Noise Control of Discrete Tones

4 – 1987 Windows to FFT Analysis (Part II)
Acoustic Calibrator for Intensity Measurement Systems

3 – 1987 Windows to FFT Analysis (Part I)

2 – 1987 Recent Developments in Accelerometer Design
Trends in Accelerometer Calibration

1 – 1987 Vibration Monitoring of Machines

(Continued on cover page 3)

Technical Review

No. 1 – 1999

Contents

Editor: Harry K. Zaveri Photographer: Peder Dalmo

Characteristics of the Vold-Kalman Order Tracking Filter

S. Gade, H. Herlufsen, H. Konstantin-Hansen, H. Vold*

Abstract

In this article the filter characteristics of the Vold-Kalman Order Tracking Filter are presented. Both frequency response as well as time response and their time-frequency relationship have been investigated. Some guidelines for optimum choice of filter parameters are presented.

The Vold-Kalman filter enables high performance simultaneous tracking of orders in systems with multiple independent shafts. With this new filter and using multiple tacho references, waveforms, as well as amplitude and phase may be extracted without the beating interactions that are associated with conventional methods. The Vold-Kalman filter provides several filter shapes for optimum resolution and stop-band suppression. Orders extracted as waveforms have no phase bias, and may hence be used for playback, synthesis and tailoring.

Résumé

Cet article présente les caractéristiques du filtrage Vold-Kalman applicable pour les suivis d'ordres. Y sont considérées la réponse en fréquence, la réponse temporelle et les relations fréquence-temps. Quelques conseils et idées directives sur le paramétrage optimal du filtre y sont également donnés.

Le filtrage Vold-Kalman permet d'effectuer un suivi d'ordres simultané et très performant pour l'analyse de systèmes multi-axiaux. Associé à l'utilisation de multi-références tachymétriques, ce nouvel outil permet d'extraire les données module, phase et formes d'onde sans les perturbations et les phénomènes de battement observés avec les méthodes conventionnelles. Diverses formes de filtre permettent l'obtention d'une résolution toujours opti-

* Vold Solution Inc., USA

male et la suppression de la bande d'arrêt. Extraits comme formes d'onde sans erreur sur la phase, les ordres peuvent être réutilisés pour la relecture, la synthèse et l'optimisation des données.

Zusammenfassung

Dieser Artikel stellt die Filtercharakteristiken des Vold-Kalman-Filters für Ordnungsanalyse vor. Untersucht wurden Frequenzgang und Zeitcharakteristik sowie die Zeit-Frequenz-Beziehung. Es werden Hinweise zur optimalen Auswahl von Filterparametern gegeben.

Das Vold-Kalman-Filter erlaubt eine präzise simultane Ordnungsanalyse in Systemen mit mehreren voneinander unabhängig rotierenden Wellen. Mit dem neuen Filter können unter Verwendung mehrerer Referenz-Tachogeber die Ordnungsverläufe sowie Amplituden und Phasen ohne die mit traditionellen Methoden verbundenen Schwebungseffekte ermittelt werden. Vold-Kalman liefert verschiedene Filterformen, um optimale Auflösung und Selektivität zu erreichen. Als Wellenformen extrahierte Ordnungen besitzen keine systematischen Phasenfehler und sind deshalb für Playback, Synthese und "Tailoring" geeignet.

Introduction

Vold and Leuridan [1] introduced in 1993 an algorithm for high resolution, slew rate independent order tracking based on the concepts of Kalman filters. Kalman filters have been employed successfully in control and guidance systems since the sixties, with particular applications to avionics and navigation [8,9]. The main feature of the filters is accurately tracking of signals of known structure among noise and other signal components with different structure. The new algorithm has been successful as implemented in a commercial software system in solving data analysis problems previously intractable with other analysis methods. At the same time certain deficiencies have surfaced, prompting the development of an improved formulation, in particular the capability of being able to control the frequency and the time response of the filter and to separate close and crossing orders [3].

This article gives an introduction to the new Vold-Kalman algorithm, presents the frequency and time response of the filters and their time-frequency relationship and gives some examples of their applications using PULSE, the Brüel & Kjær, Multi-analyzer System Type 3560 [4].

Overview of Methods for Analysis of Non-Stationary Signals

A number of traditional analysis methods can be used for the analysis of non-stationary signals and they can roughly be categorized as follows:

1) Divide into Quasi-stationary segments by proper selection of analysis window
   a) Record the signal in a time buffer (or on disk) and analyze afterwards: Scan Analysis
   b) Analyze on-line and store the spectra for later presentation and post-processing: Multifunction/multibuffer measurements
2) Analyze individual events in a cycle of a signal and average over several cycles: Gated measurements and analysis
3) Sample the signal according to its frequency/RPM variations (adaptive data resampling): Order tracking measurements
4) Analysis using Autoregressive Signal Modelling: Maximum Entropy Spectral Analysis [11].

The procedure used for Vold-Kalman order tracking analysis (adaptive filtering, where the presumed model of the signal is not fixed in time or frequency content, but automatically adapts itself as the speed of the device under test changes) is as described in 1a) above, i.e. a post-processing procedure based on time data.

Order Tracking Analysis

Order tracking is the art and science of extracting the sinusoidal content of measurements from acousto-mechanical systems under periodic loading/excitation. Order tracking is used for troubleshooting, design and synthesis [5, 18].

Each periodic loading produces sinusoidal overtones, or orders/harmonics, at frequencies that are multiples of that of the fundamental tone (RPM). The orders may be regarded as amplitude and phase modulated carrier waves that vary in frequency. Many practical systems have multiple shafts that may run coherently through fixed transmissions, or partially related through belt slippage and control loops, or independently, such as when a cooling fan operates in an engine compartment.

In order analysis we focus on machine revolutions rather than on time as the base for the signal analysis. Thus in the spectrum domain the focus is on orders rather than frequency components.

Traditional Analysis Techniques for Run-up/ Run-down Tests

One of the main applications of order tracking is analysis of run-ups and run-downs. Investigation of the system responses and dynamic behaviour at the various rotational speeds is a key element in design, troubleshooting, product testing and quality control. Depending on the information required from the test, different analysis techniques can be applied.

The most simple is determination of the acoustic response in terms of the overall Linear, A, B or C weighted level as a function of RPM. This is often used in product testing for comparison with reference (tolerance) curves. No diagnostic information is obtained.

"Next level" of analysis is the inclusion of spectral information. In acoustic testing 1/1-octave or 1/3-octave spectra are often used in order to get the spectral content in constant percentage filter bands as a function of rotational speed (constant percentage bandwidth means that the bandwidth is proportional with the frequency). These can reveal frequency regions with annoying resonances and they relate to the human perception of the radiated noise. Information about the individual orders cannot be extracted except for the lowest harmonics with 1/3-octave filters. Fig.1 shows the contour plot of the acoustic response during a run-up of a motor analyzed in 1/3-octaves. The 1st (and to some degree the 2nd) order is identified together with regions of high response levels. Fig.2 shows the overall level as well as some individual 1/3-octave bands as a function of RPM. More information about the lower harmonic order components could be obtained by going to for example 1/12-octave filter bandwidth. Real-time 1/12-octave filters, however, require more DSP (Digital Signal Processing) power in the system.

More advanced acoustic processing is to use a Loudness Analyzer and store non-stationary Specific Loudness as a function of RPM, [14]. Non-stationary Loudness gives a much better model of the human hearing system and takes into account that the sensitivity of the human ear is not the same for all frequencies and levels as well as the effect of temporal and frequency masking.

In order to resolve the various orders in the frequency domain, narrowband frequency spectra (FFT without tracking) could be applied. FFT gives the spectral information in constant bandwidth (same bandwidth at all frequencies and RPMs) and facilitates identification of harmonic families when presented on a linear frequency axis. This enables diagnosis and source identification.The advantage of using FFT without tracking is that it does not cost very much in terms of DSP power. Another advantage is that one FFT analyzer can relate the analysis to more tacho signals: multi-shaft analysis. A disadvantage is that

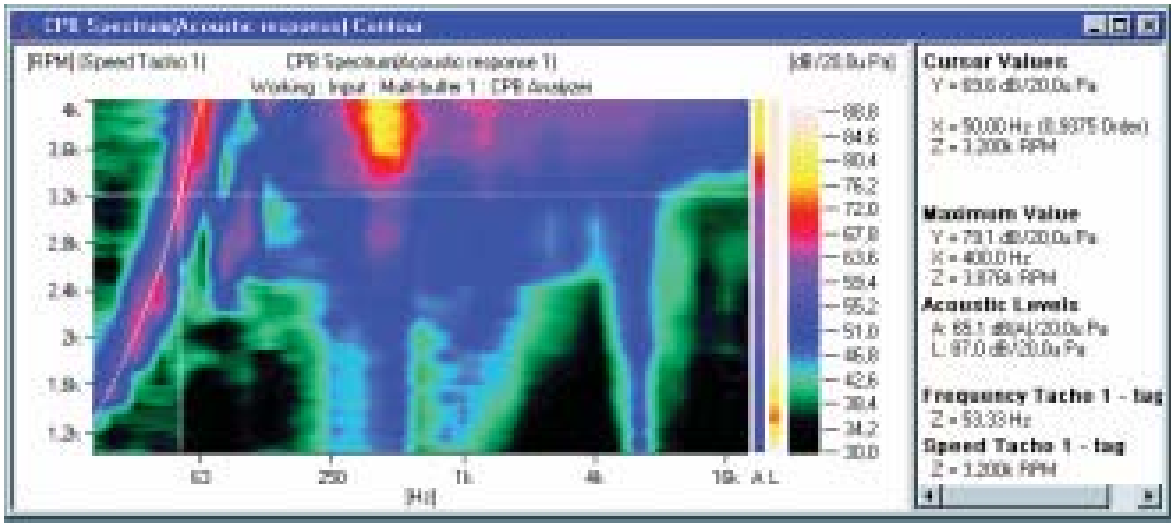

Fig. 1. 1/3-octave colour contour plot (maximum interpolation used) of the acoustic response during run-up

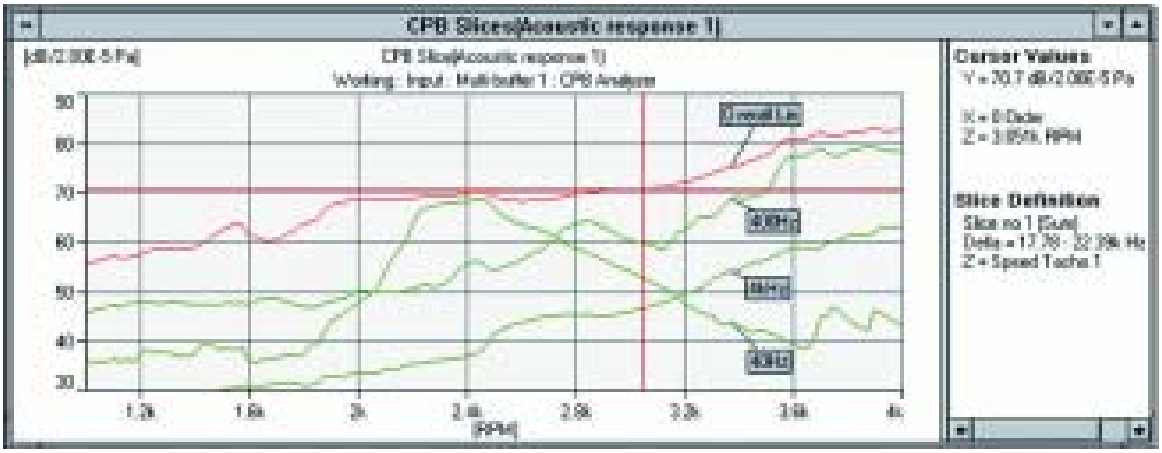

Fig. 2. Selected 1/3-octave bands and overall linear level of acoustic response as functions of RPM

the smearing of the individual (and especially the higher) order components in the frequency spectra will appear if the run-up/run-down is fast. This is due to the fact that each FFT spectrum represents a certain time window and therefore a certain change of the rotational speed. Another aspect is that rather large Fourier transforms (many lines in the FFT) are required in cases where the test is running over a wide speed (RPM) range and higher harmonics have to be included in the analysis. Example: RPM range from 600 RPM (10 Hz) to 6000 RPM (100 Hz), 16 orders included in the spectra (i.e. min. 16 x 100 Hz = 1.6 kHz frequency span) and a resolution of 2 Hz (5 FFT lines per

order at 600 RPM) will require 800 FFT lines in the analysis (2 Hz resolution with a frequency span of 1.6 kHz).

Fig. 3 shows the contour plot of an FFT analysis of the same acoustic response as in Fig. 1. The harmonic family of the fundamental periodic loading is easily identified. Resonance frequencies excited by the various harmonic orders appear on vertical lines parallel to the RPM axis. Fig. 4 shows the first 4 harmonics and the total level in the selected frequency span, as a function of RPM. This information is obtained by slicing in the contour plot (post-processed in "real-time" during the test) or by pre-processing, i.e. directly measured by the FFT analyzer during the run-up/run-down. Both order – as well as frequency-slices can be measured/extracted using these methods.

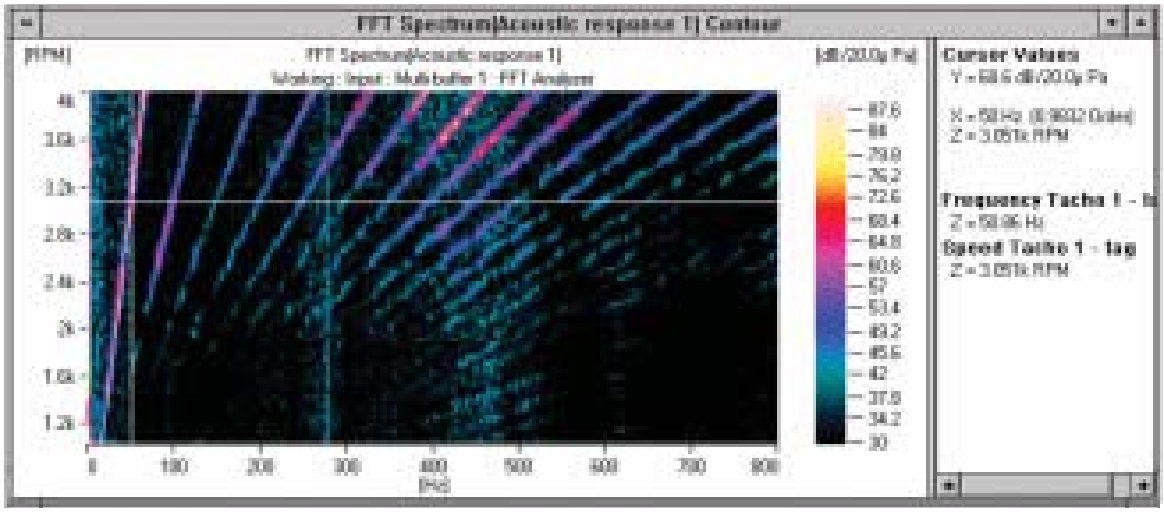

Fig. 3. Contour plot of the FFT spectra of the acoustic response as function of RPM

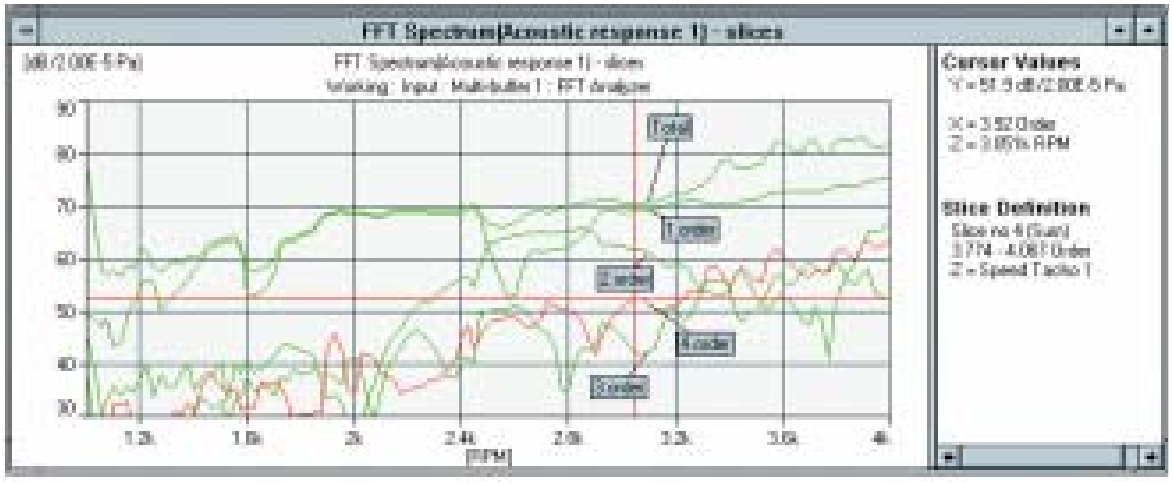

Fig. 4. Selected orders and total level (in the frequency span) as functions of RPM

The above mentioned disadvantages can be overcome by use of tracking. The tracking technique uses the instantaneous RPM values for calculation of the samples referenced to the revolution of the rotating shafts instead of the time clock, see e.g. [5]. Fourier transform of the revolution based samples results in order spectra instead of frequency spectra and harmonic orders related to the measured RPM remains in fixed lines in the order spectrum. This means that smearing of the order related components is avoided and order components, which might have been smeared out in a frequency spectrum, can be identified. The number of lines required in the order spectra for a certain test is less than the number of lines needed if frequency spectra were used. Example: 20 orders is analyzed with a resolution of 0.2 order (5 lines per order, giving possibility to identify inter-harmonic components) by use of 100 line order spectra independent of the speed range. The price to pay is that the real-time tracking algorithms require more DSP power than the "normal" FFT analysis.

Fig. 5 shows the contour plot of order spectra of the same acoustic response as in Fig. 1 and Fig. 3. The orders appear on vertical lines parallel to the RPM axis whereas resonances appear on hyperbolic curves (fixed frequency curves indicated by the cursor). Slices of the first 10 harmonics and the total level as a function of RPM is shown (as a waterfall plot) in Fig. 6. The order slice results obtained by the frequency analysis and the order analysis are the same.

In product testing there is often a requirement of having the results in real-time (on-line) containing information of both individual orders, overall levels (Linear, A, B or C weighted) and in some cases 1/1- or 1/3-octave bands as well. This can only be obtained using a combination of the mentioned techniques. The key issue, in order to reduce the test time and have consistency of data in the various analyses is to perform the analyses simultaneously. This is the case in the results illustrated in Fig. 1 through Fig. 6 where the Brüel & Kjær PULSE, Multi-analyzer System Type 3560 is used. Four analyzers are used in parallel: A tachometer (for RPM calculations), a 1/3-octave analyzer (1/3-octaves and overall levels), an FFT analyzer (frequency spectra) and an order analyzer (order spectra) giving all the results simultaneously. A loudness analyzer can be included as well. In this example only one tachometer signal is used. In multiaxle applications the different tachometer signals should be applied to the tachometer. The scaling of the RPM axis and the calculation of the order slices can then be referenced to the different rotation speeds (RPMs). If tracking is used (as in Fig. 5 and Fig. 6) an order analyzer would have to be defined for each reference tachometer signal.

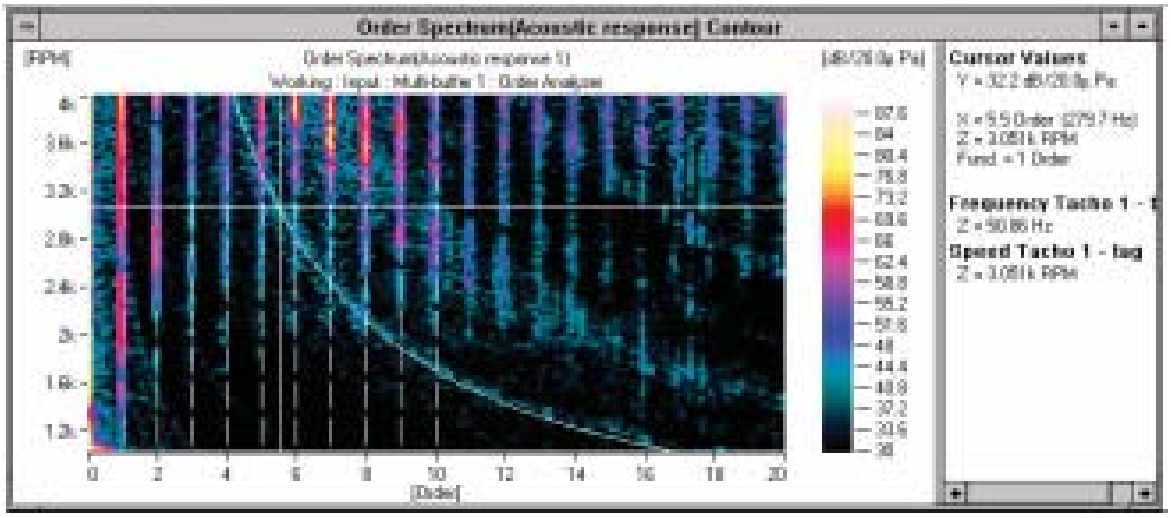

Fig. 5. Contour plot of real-time order tracking spectra (resampling technique) of the acoustic response

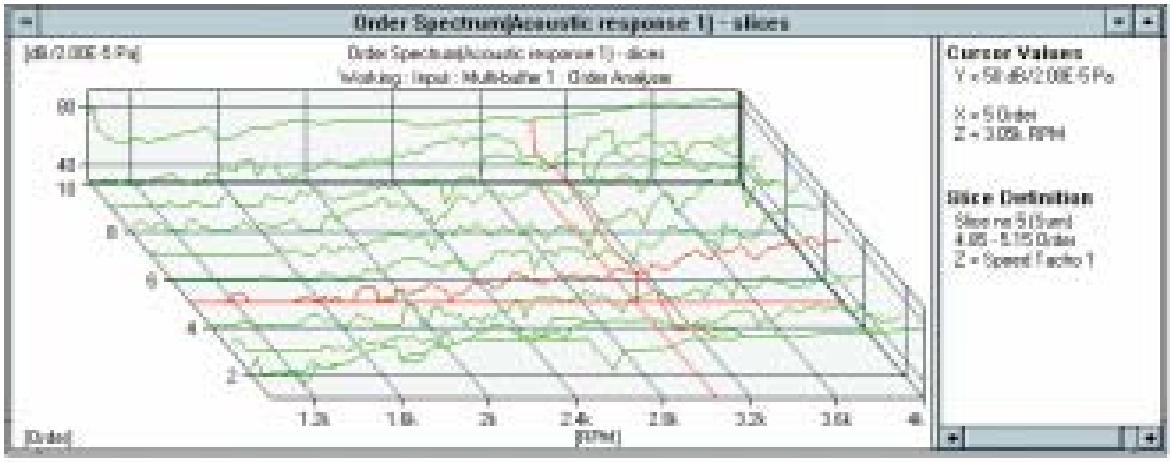

Fig. 6. First 10 harmonics and the total level (in the span of 20 orders), from real-time order tracking spectra, as functions of RPM (shown as a waterfall plot)

These analysis techniques can be applied in real-time (on-line) which means that the results are obtained during the test. They are based upon conventional frequency (Fourier) analysis that means that the resolution in the time domain is linked to the resolution in the frequency domain and vice versa. This gives a limitation of how accurate phenomena can be identified in both domains in the same analysis. This is also referred to as the uncertainty principle. For FFT analysis the relation is written as $\Delta f \times T = 1$, where T is the record length ("resolution" in time domain) and Δf is the line spacing in the spectrum ("resolution" in frequency domain). If the changes in the signals are

too rapid we will not be able to follow (analyze) these changes using these techniques. The real-time order tracking technique, mentioned above, is based on resampling and there is a limitation of how fast the speed (RPM) is allowed to change (also called slew rate limitation).

These limitations are examples of where the Vold-Kalman tracking filter can be used, rendering a comprehensive set of analysis tools. It minimizes the resolution problems and has no slew rate limitations.

Applications of Vold-Kalman Order Tracking Filtering

The Vold-Kalman algorithm enables simultaneous estimation of multiple orders, effectively decoupling close and crossing orders, e.g., separating drive shaft orders from wheel orders in suspension tuning. Decoupling is especially important for acoustics applications, where order crossings cause transient beating events. The new algorithm allows for a much wider range of filter shapes, such that signals with sideband modulations are processed with high fidelity. Finally, systems subject to radical RPM changes, such as transmissions, are tracked also through the transient events (e.g. gear shifts) associated with abrupt changes in inertia and boundary conditions. The goal of order tracking is to extract selected orders in terms of amplitude and phase, called Complex Orders or Phase Assigned Orders, or as waveforms. The order functions are extracted without time delay (no phase shift), and may hence be used in synthesis applications for sound quality, e.g. removal of nuisance orders and laboratory simulations. Other applications include multiplane balancing, and measurements of Operational Deflection Shapes, ODS.

Fundamental Notions and Equations

Mechanical systems under periodic loading, such as those with one or more rotating shafts will respond in measurements with a superposition of sine waves whose frequencies are integer multiples of the fundamental excitation frequencies. Notice that this also applies to the limit cycle response of non-linear systems. As the periodic loadings change their speed, the responses will also change their frequencies accordingly. Since mechanical systems normally have transfer characteristics dependent upon frequency, the amplitude and phase of these sine waves will typically also change as the periodic loadings change their speed. The sine waves whose frequencies are constant multiples

of an underlying periodic loading are said to be harmonics or orders of that loading, also when the multiple is fractional due to gears or belt drives.

It is often helpful to visualize an order as an amplitude/phase modulated radio signal. The underlying sine wave whose frequency is a multiple of the fundamental periodic phenomenon would be the carrier wave, while the slowly varying amplitude and phase function that modulates the carrier wave is the radio program. A radio receiver demodulates the signal by removing the carrier wave and playing the modulation function, also known as the (complex) envelope. Now, in mechanical systems, the carrier wave may continually change its frequency, making the orders similar to amplitude modulated spread spectrum radio signals.

The goal of order tracking is to extract selected orders in terms of amplitude and phase or as real time series. These entities will in general be estimated as functions of time to allow for any pattern of speed or axle RPM variations.

Phasors and Complex Envelopes

The carrier wave of an order can be visualised as a phasor, which is a complex oscillator with an instantaneous frequency proportional to a constant multiple of the underlying axle speed as in the equation

$$\Theta_k(t) = \exp\left(2\pi k i \int_0^t f(u)du\right) \tag{1}$$

where the integral of frequency gives the angle travelled by the axle up to the current time, k is the order number and $i = \sqrt{-1}$. Note that the phasor is always on the complex unit circle.

The amplitude modulated complex order is now given as the product $A_k(t)\ \Theta_k(t)$ where $A_k(t)$ is the complex envelope. These complex orders must occur in complex conjugate pairs to sum to a real signal, such that the total superposition $X(t)$ of orders relative to an axle can be written as

$$X(t) = \sum_k A_k(t)\Theta_k(t) \tag{2}$$

where k runs over all positive and negative multiples of the underlying axle speed.

Time Variant Zoom

The expression for the phasor (1) implies the functional relationship

$$\Theta_k(t)\Theta_j(t) = \Theta_{k+j}(t) \tag{3}$$

In particular, inspection of equation (1) shows that $\Theta_0(t) \equiv 1$. When the axle speed has been estimated as a function of time, equations (2) and (3) then show that we can centre a designated order at DC (zero frequency) by the *time variant zoom transform*

$$\Theta_{-j}(t)X(t) = A_j(t) + \sum_{k \neq j} A_k(t)\Theta_{k-j}(t) \tag{4}$$

The low frequency complex envelope $A_j(t)$ has now been straightened, and may, for example, be extracted in the time domain by any suitable lowpass filter. This *super-heterodyning* process is similar to the tracking of an amplitude modulated spread spectrum radio source.

Using traditional tracking algorithms the centre frequency of a bandpass tracking filter is controlled by the instantaneous RPM. The filter AC output is then detected (squared and averaged) into a "slowly" varying DC using, for example, a traditional RMS detector, with all its well known limitations, among those – averaging time dependent ripple in the output as well as loss of phase information. For the Vold-Kalman processing, the order of interest is frequency shifted (or zoomed) to DC, a shift which is controlled by the instantaneous RPM and then followed by a lowpass filtration which replaces the bandpass filtering process. Thus there is no need for any further detection; i.e. the Vold-Kalman filtration includes a simultaneous envelope detection of both magnitude and phase. Order Waveforms are then obtained by remodulating the complex orders by the order frequency carrier wave (given by the RPM profile), i.e. the complex orders are heterodyned from DC to its original frequency location.

Vold-Kalman Filter

The basic idea behind the Vold-Kalman filter is to define local constraints that state that the unknown complex envelopes are smooth and that the sum of the orders should approximate the total measured signal. The smoothness

condition is called the structural equation, and the relationship with the measured data is called the data equation. The somewhat ambiguous notation $X(n\Delta t) = X(n)$, where Δt is the sampling time increment, is used in this article to simplify the mathematical exposition.

Structural Equations

The complex envelope $A_j(t)$ is the low frequency modulation of the carrier wave $\Theta_j(t)$. Low frequency entails smoothness, and one sufficient condition for smoothness is that the function locally can be represented by a low order polynomial. This condition can be expressed in continuous time using multiple differentiation as

$$\frac{d^s A_j(t)}{dt^s} = \varepsilon(t) \tag{5}$$

where $\varepsilon(t)$ represents higher order terms. The same constraint can be applied to sampled data by using the difference operator such that

$$\nabla^s A_j(n) = \tilde{\varepsilon}(n) \tag{6}$$

Note that the difference operator of a given order annihilates all polynomials of one order less. Equation (6) is called the structural equation when the right hand side $\tilde{\varepsilon}(n)$ is regarded as noise or error. This complex equation will be satisfied in an approximate sense for all discrete time points in the data set.

The structural difference equation in the first generation of the Vold-Kalman algorithm is a real second order equation for the real modulated waveform

$$X_j(n) = 2\mathrm{Re}(A_j(n)\Theta_j(n)) \tag{7}$$

that requires a demodulation through the Vandermonde equations to find the amplitude and phase, see [1]. This operator also only annihilates the constant polynomial.

Data Equation

The structural equation only enforces the smoothness conditions on the estimates of the complex envelopes, such that we need an equation that relates the estimates to the measured data. The simplest such condition is to state that the sum of the orders differs only by an error term from the measured data as expressed in the equation

$$X(n) - \sum_{j \in J} A_j(n)\Theta_j(n) = \tilde{\delta}(n) \tag{8}$$

where the summation is for a desired subset of orders.

The above equation (8) is called the data equation when the right-hand side $\tilde{\delta}(n)$ is regarded as noise or error. This equation will also be enforced in an approximate sense for all sampled data points.

Decoupling

When several orders are estimated simultaneously, equation (8) ensures that the total signal energy will be distributed between these orders, and together with the smoothness conditions of the structural equation (6) this enforces a decoupling of close and crossing orders as is demonstrated in the examples. The mathematics of this procedure is quite analogous to the repeated root problem in modal analysis, see, [7]. When orders coincide in frequency over an extended time segment, the allocation of energy to such orders is poorly defined, and numerical ill conditioning may ensue. Widening the filter bandwidth is one possible remedy in this case.

Example of Tacho Processing

Any method with high resolution needs proper controls, and for the Vold-Kalman filter this means a very accurate estimation of the instantaneous RPM such that the tracking filter will follow the peak of the order functions instead of extracting data from the foothills. The methodology that has been chosen for the Vold-Kalman filter is that of fitting cubic splines in a least squares sense to the table of level crossings from a tacho waveform. Choice of other possible methods is discussed in [1]. Tacho processing is explained in more details later.

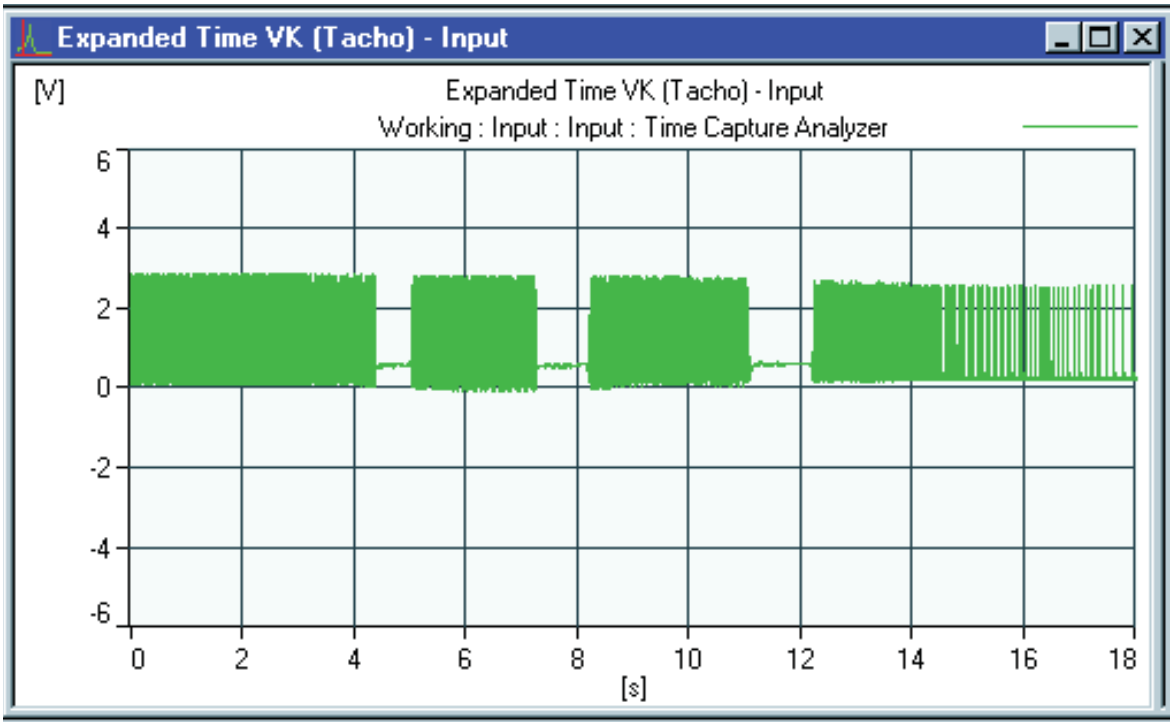

Fig. 7. Corrupted tacho waveform, Run-down from 5200 RPM to 400 RPM

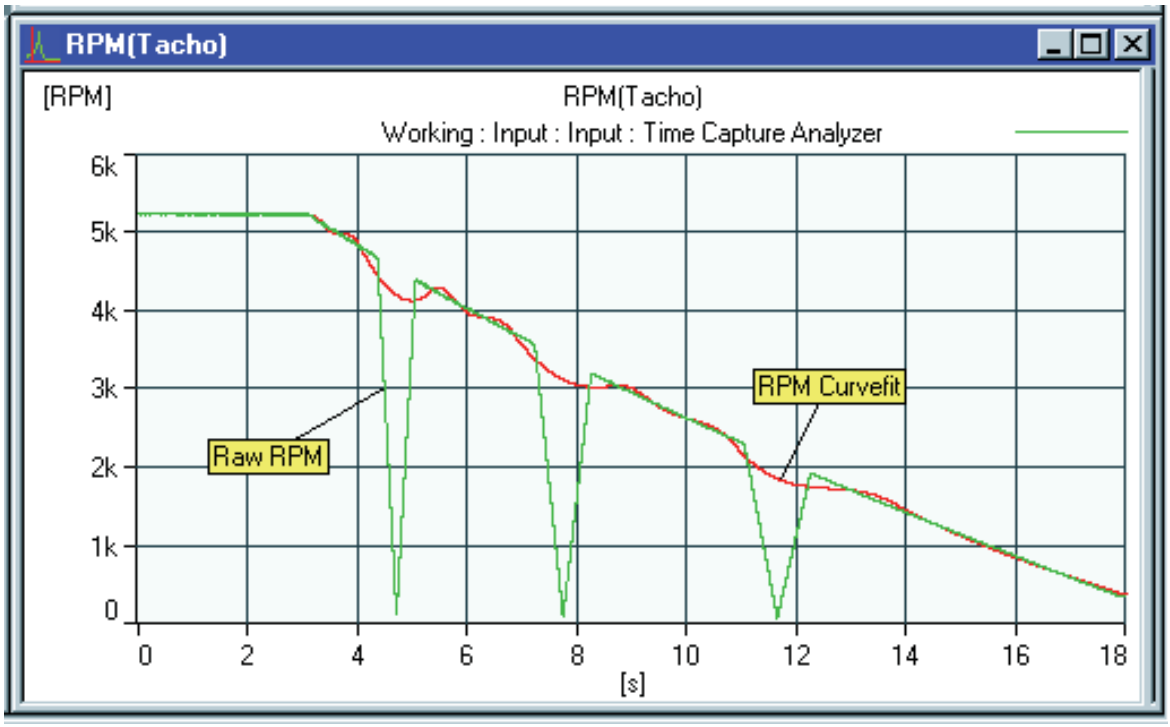

Fig. 8. Raw data and spline fit

The spline fit enables automatic rejection of outlying data points with a subsequent refit on a censored table of level crossings. The spline fit and censoring process capability is illustrated by the corrupted tachometer signal from a 5200 RPM to 400 RPM run-down lasting for about 15 s. There are three dropouts with a total duration of 15% of the total measurement time as shown in Fig. 7. The raw level crossing table and spline fit without rejection is shown in Fig. 8. The fitted data is then compared with the raw table, the largest deviants (in this case 1% of the raw RPM table has been specified for rejection) are censored and a refit is performed, with the clean results depicted in Fig. 9. As a result the three "wild" RPM points have been removed and the spline fit is sufficiently stiff to straddle the empty sections. This is a fully automatic process, often obviating the need for manual tacho signal repair. Notice that the raw RPM profiles have been drawn as curves, i.e. with straight-line connections between the table values, both without and with rejections shown in Figs. 8 & 9.

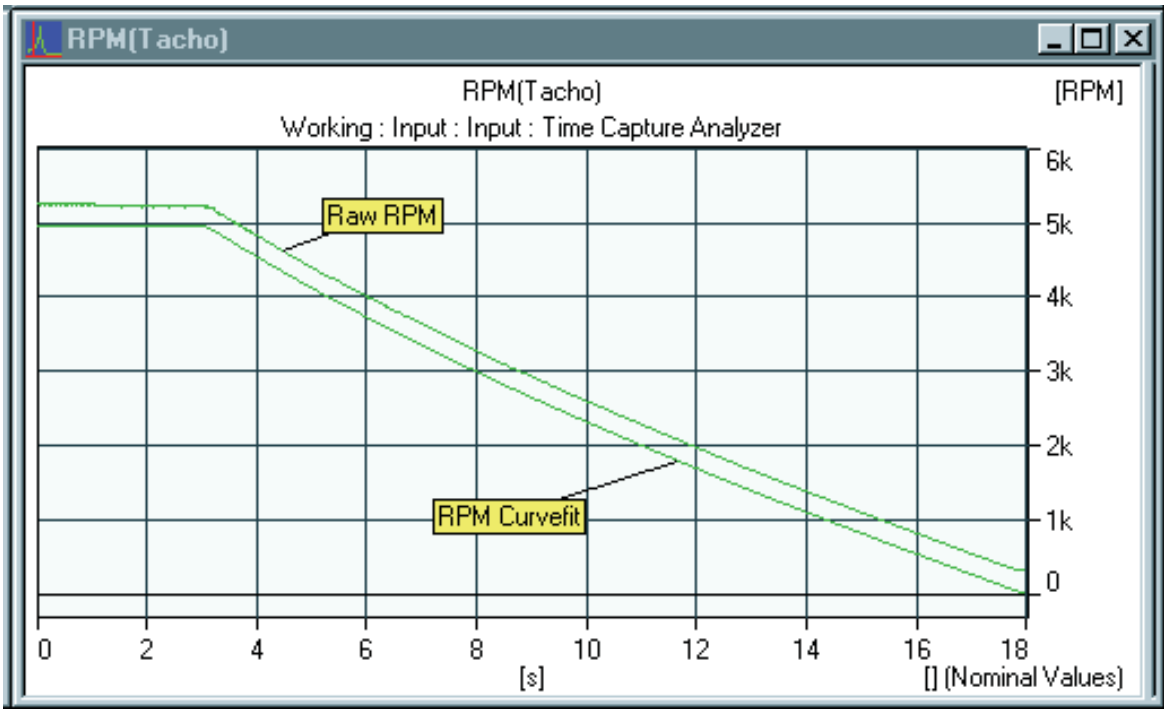

Fig. 9. Censored Data with Corrected Spline Fit (curves offset for ease of comparison)

Vold-Kalman Filter Process, Step by Step – an Example

To illustrate the ease of use of the Vold-Kalman filter process as implemented in the Brüel & Kjær PULSE, Multi-analysis System Type 3560, a run-up measurement on a small single shaft electrical motor has been performed. Fig. 10 shows the vibration response signal, which was recorded together with a tacho signal. A 1.6 kHz frequency range and a total recording of 20 s have been selected using a PULSE Time Capture Analyzer [17]. The number of samples recorded is 81 920 in each channel. 18 s of the recorded signal was extracted for Vold-Kalman tracking using a delta cursor.

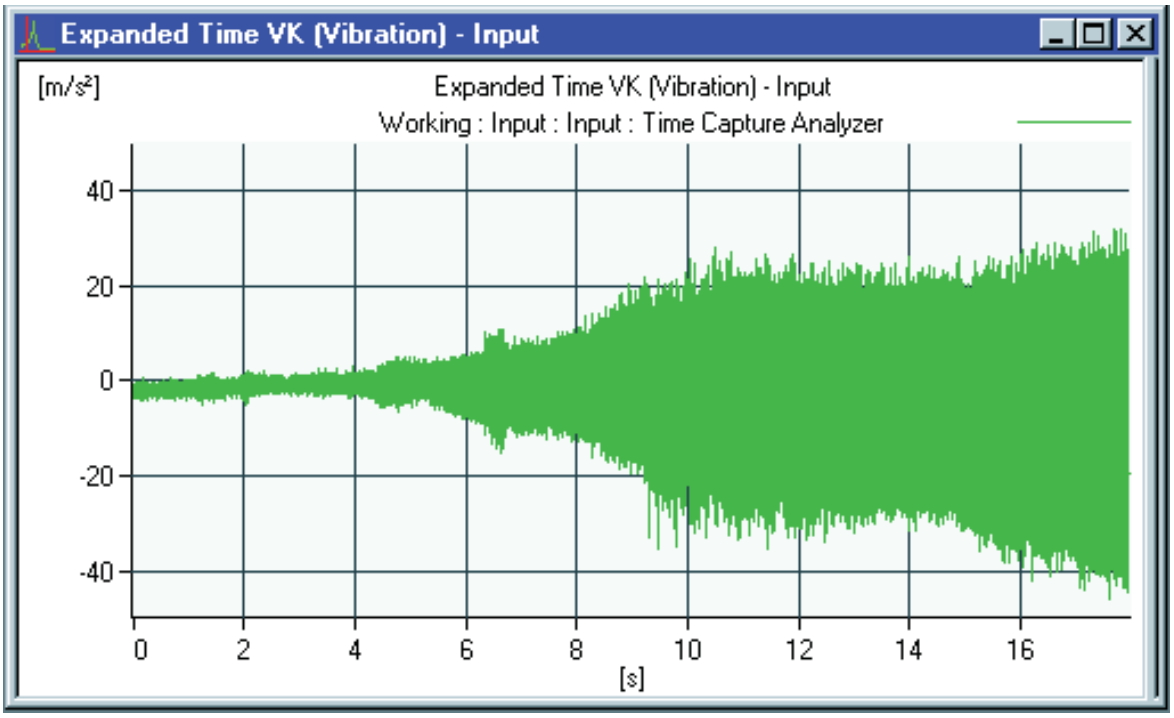

Fig. 10. Vibration time signal of the run-up

a) Overview of the Event using Fourier Analysis

The first step is to use conventional techniques in order to gain some insight in the harmonic orders of interest, gearshifts etc. Fig. 11 shows a contour plot of an STFT (Short Time Fourier Transform) of the vibration signal. The record length of each transform is set to 125 ms (512 samples) resulting in 200 lines in the frequency domain (line spacing Δf of 8 Hz). An overlap of 66% is used resulting in a multi-buffer of 500 spectra covering the selected 18 s. From the contour plot it is revealed that the dominating orders are nos. 1, 3, 9 and 10 and as expected, no gearshift is present.

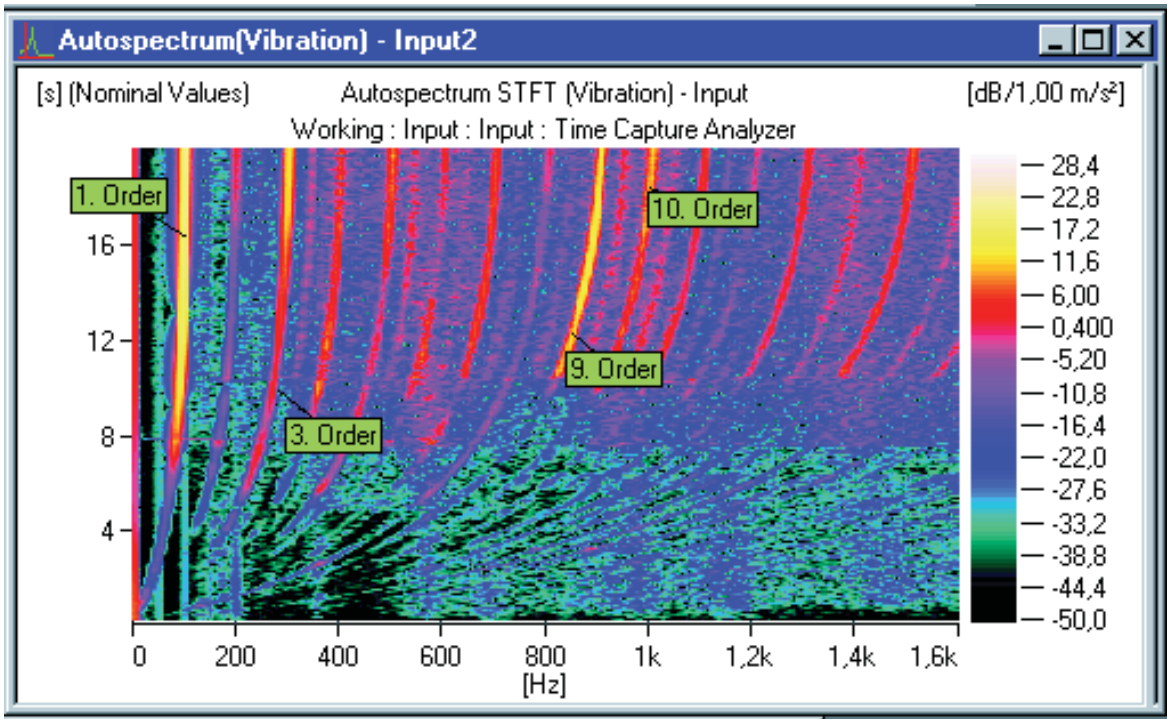

Fig. 11. An STFT of the vibration signal

b) Tacho Processing

As mentioned earlier any method with high resolution needs proper controls, and for the Vold-Kalman filter this means a very accurate estimation of the instantaneous RPM such that the tracking filter will follow orders correctly. The method of fitting cubic splines to the table of level crossings from a tacho waveform gives an analytic expression of the RPM as a continuous function of time, i.e. an instantaneous or "sample by sample" estimate of RPM, with true tracking of the shaft rotation angle for phase fidelity. As a consequence Vold-Kalman filtering will produce a complex order value for every measurement sample point. Fig. 12 shows the tacho settings, including slope, hysteresis and gearing that defines the table of RPM values, each of them positioned in time exactly midway between two consecutive tacho pulses as shown in Fig. 8.

The tacho table is divided into a number of segments, in which a cubic least squares spline fit, allowing for one local minimum and one local maximum, is applied in order to smooth the data. Fewer the segments, the stiffer and smoother the interpolation would be. The more segments are chosen, the closer the interpolation will fit the data points. In practice one should increase the

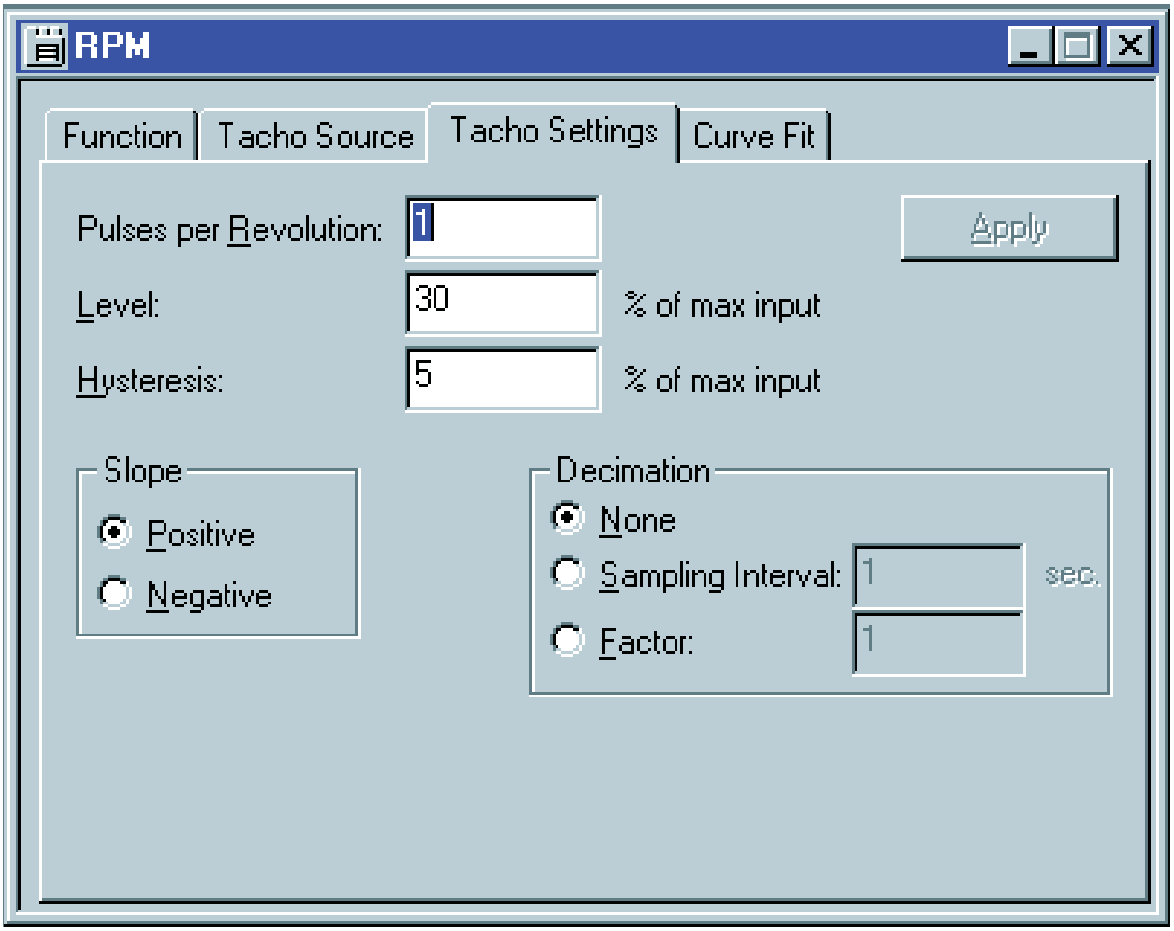

Fig. 12. Tacho setting property page

number of segments until a reasonable match to the raw RPM is obtained. Too many segments might fit non-physical variations (noise) in the raw RPM. Continuity and first derivative continuity constraint requirement is applied between segments. There is also the option of specifying hinge points (singular events) in the spline fit, such that sudden changes in inertial properties can be tracked, as in the case of clutching and gearshifts by relaxing the first derivative continuity at shift points. The operator identifies the exact locations of hinge points by expanding the RPM profiles for detailed visual inspection.

The spline fit also permits automatic rejection of outlying data points (such as tacho dropouts) with a subsequent refit on a censored table of level crossings as mentioned earlier. The Curve Fit property page is shown in Fig. 13.

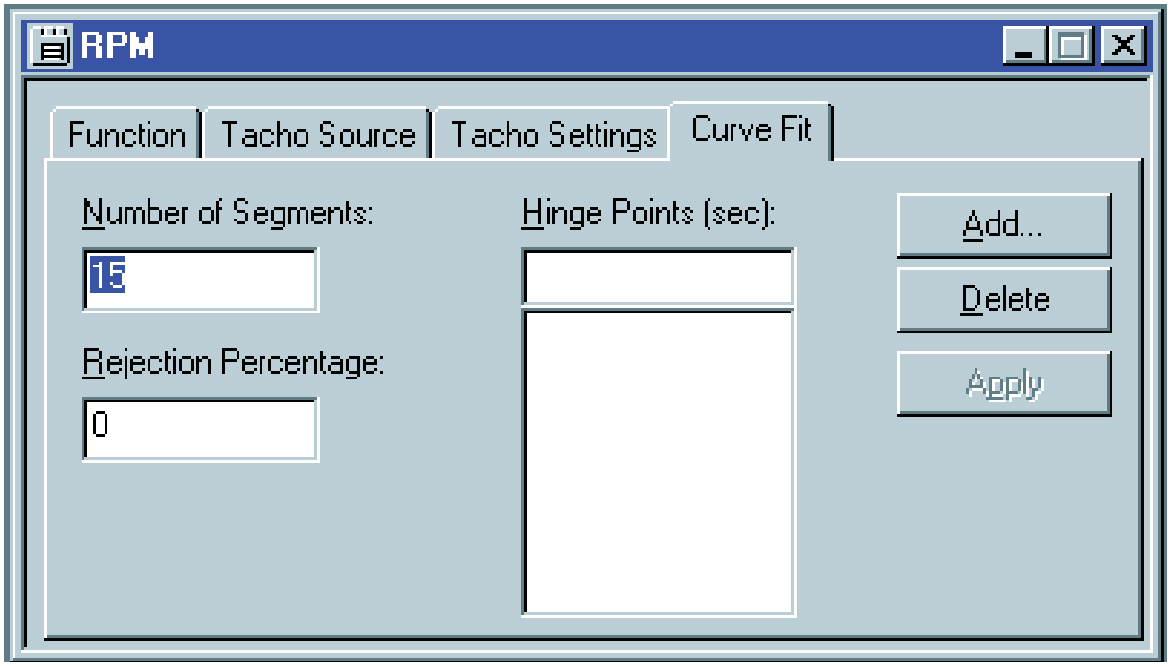

Fig. 13. Tacho table Curve Fit property page

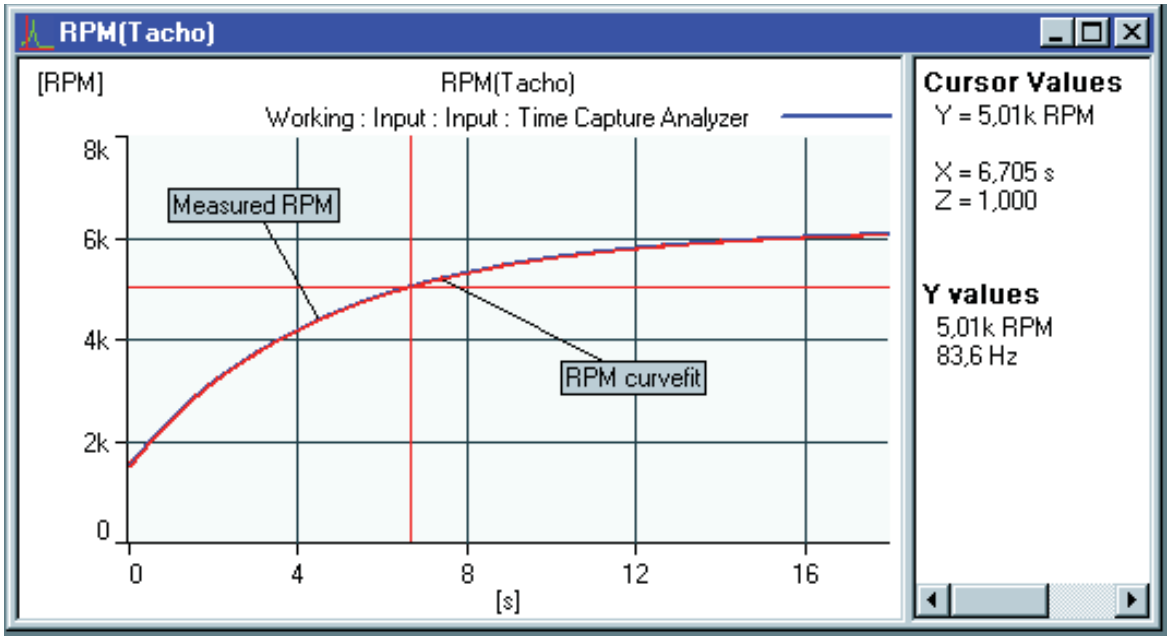

Fig. 14. Comparison of the measured (raw, tabular) and curve fitted RPM profiles

Fig. 14 shows a superimposed graph of the measured and the curve fitted RPM profiles. The maximum slew rate in this case is seen to be approximately 800 RPM/s and the range is between 1000 RPM and 6000 RPM.

c) Vold-Kalman Filtering

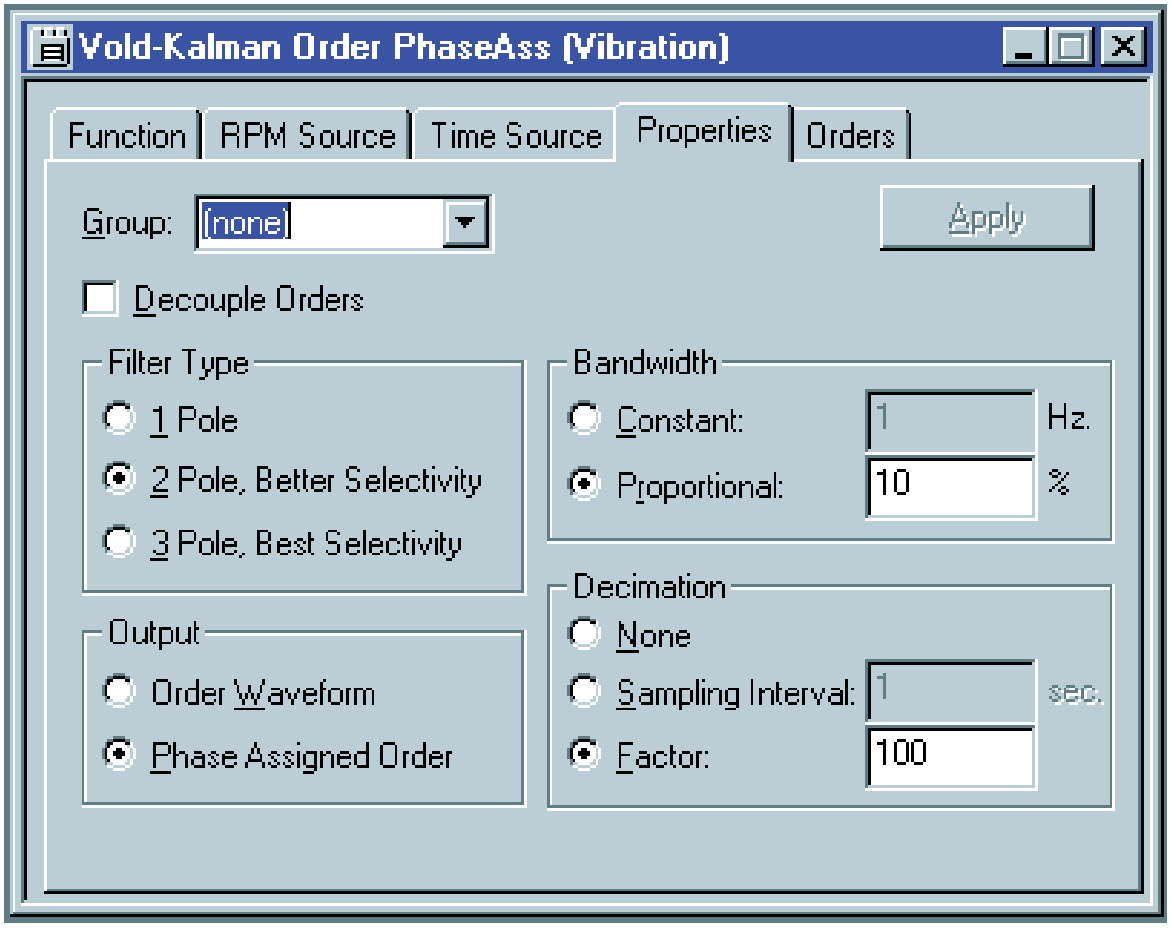

Fig. 15. Vold-Kalman filter property page

Orders can now be extracted from the signal in terms of waveforms or as Phase Assigned Orders (Complex Orders).

The Vold-Kalman filter property page is shown in Fig. 15. The computational complexity of the Vold-Kalman filter is proportional to the number of time samples and to the number of orders to be extracted, but also to some degree depends on filter type, output, bandwidth and decimation. For example, the computation time for a three-pole filter is 10% longer than for a two-pole filter.

When decoupling is used, however, the computational cost can be high, since constraint conditions are being enforced between the order function estimates.

Fig. 16 shows the waveform of the 1st, 3rd, 9th and 10th order extracted using a two-pole Vold-Kalman filter with a bandwidth of 10% (i.e. 10% of the fundamental frequency). Extracted waveforms can be played via a sound card and they can be exported as wave files. Sound Quality application is an example were this is very useful.

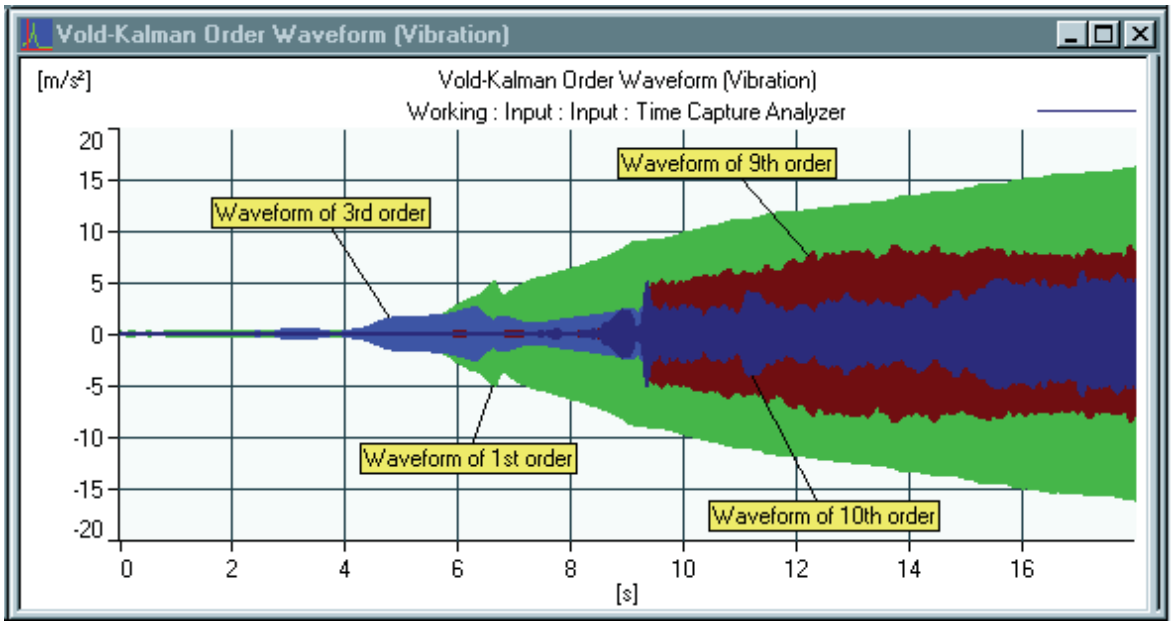

Fig. 16. Waveforms of the 1st, 3rd, 9th and 10th Order, extracted using a two-pole Vold-Kalman filter with 10% bandwidth

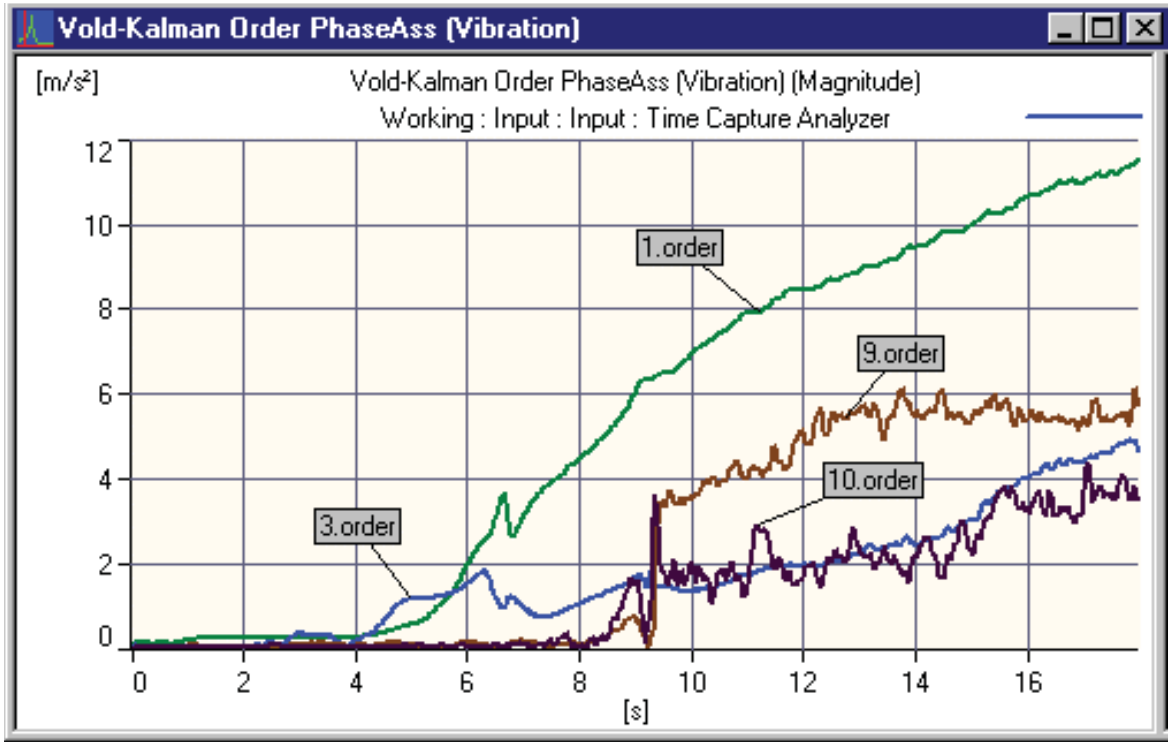

Fig. 17. Magnitude of the 4 most dominating orders as a function of time, extracted using a two-pole Vold-Kalman filter with 10% bandwidth

Extracted as Phase Assigned Orders means that the orders are determined in terms of magnitude and phase. Fig. 17 shows the magnitude of the Phase Assigned Orders of the 1st, 3rd, 9th and 10th order, which were the 4 most dominating orders. A two-pole Vold-Kalman filter with a bandwidth of 10% is used. It should be noted that the phase of the orders is highly sensitive to choice of filter bandwidth for time sections with poor signal to noise ratio. This is most evident when displaying unwrapped phase.

The Vold-Kalman analysis is a time-based analysis yielding results, Phase Assigned Orders and Waveforms as a function of time. Often it is desirable to plot the Phase Assigned Orders as a function of RPM, which can be easily done by exporting the order of interest and the RPM-profile to a spreadsheet. The magnitude of the first order is shown in Fig. 18 using MS Excel. The decimation features shown in Figs. 12 and 15 are used in this case in order to reduce the amount of data to a size, which can be handled by a spreadsheet.

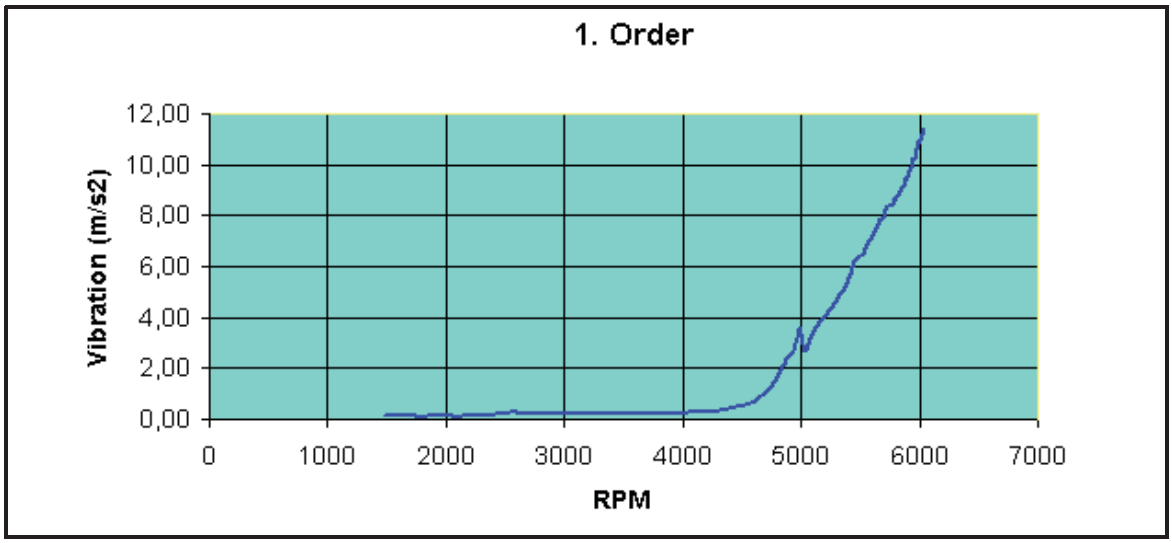

Fig. 18. Magnitude of the first order as a function of RPM, extracted using a two-pole Vold-Kalman filter with 10% bandwidth and plotted via MS Excel spreadsheet

Filter Characteristics in Frequency Domain

Bandwidth selection is done in terms of constant frequency bandwidth or proportional to RPM bandwidth (i.e. constant percentage bandwidth). The bandwidth specification in the Brüel & Kjær Vold-Kalman implementation [16] is in terms of the half – power points, i.e. 3 dB bandwidth. Bandwidth proportional to RPM is recommended for the analysis of higher harmonic orders or analysis of wide RPM ranges.

The filter shape is measured by sweeping a sine wave through a Vold-Kalman filter with a fixed centre frequency and fixed bandwidth. A sweep rate of 1 Hz/s is used for measuring the filter shapes, shown in Fig. 19, of a Vold-Kalman filter with a centre frequency of 100 Hz and a bandwidth of 8 Hz. The x-axis, which is a time axis scaled in seconds, can directly be interpreted as a frequency axis scaled in Hz (with a fixed offset). It is seen that a one-pole filter has very poor selectivity, a two-pole filter has a much better selectivity, whereas a three-pole filter provides the best selectivity. The 60 dB shape factor, i.e. the ratio between the 60 dB bandwidth and the 3 dB bandwidth is often used for describing the selectivity of a filter. The 60 dB shape factor has been measured for the one-, two- and three-pole filters for bandwidths in the range from 0.125 Hz to 16 Hz. These tests showed that the 60 dB shape factor for a given pole specification increases slightly as a function of bandwidth. The one-pole filter has a 60 dB shape factor of approximately 50 (variation from 48.8 to 50.8). The two-pole filter has a 60 dB shape factor of approximately 7.0 (variation from 6.80 to 7.07) and the three-pole filter has a 60 dB shape factor of approximately 3.6 (variation from 3.58 to 3.68). Thus the selectivity of the three-pole filter is twice as good as the two-pole filter and 14 times better than the one-pole filter. Good selectivity is important to avoid interference (or leakage) between orders.

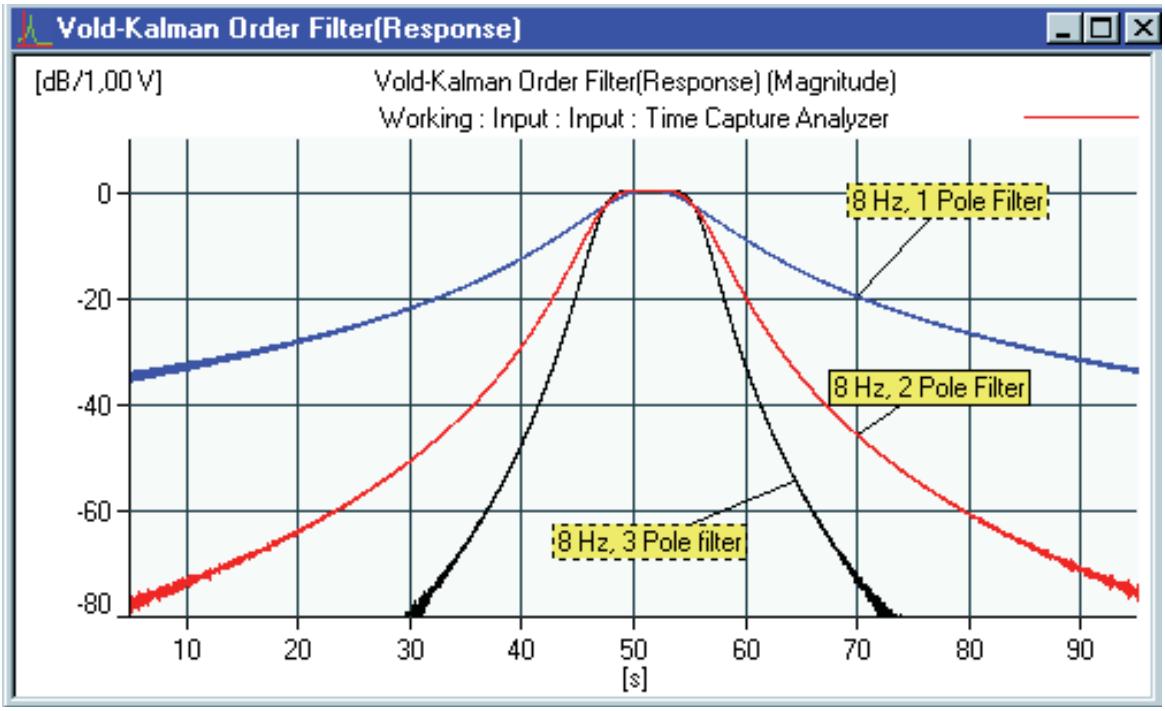

Fig. 19. Comparison of filter shapes for one-, two- and three-pole Vold-Kalman filters with a bandwidth of 8 Hz

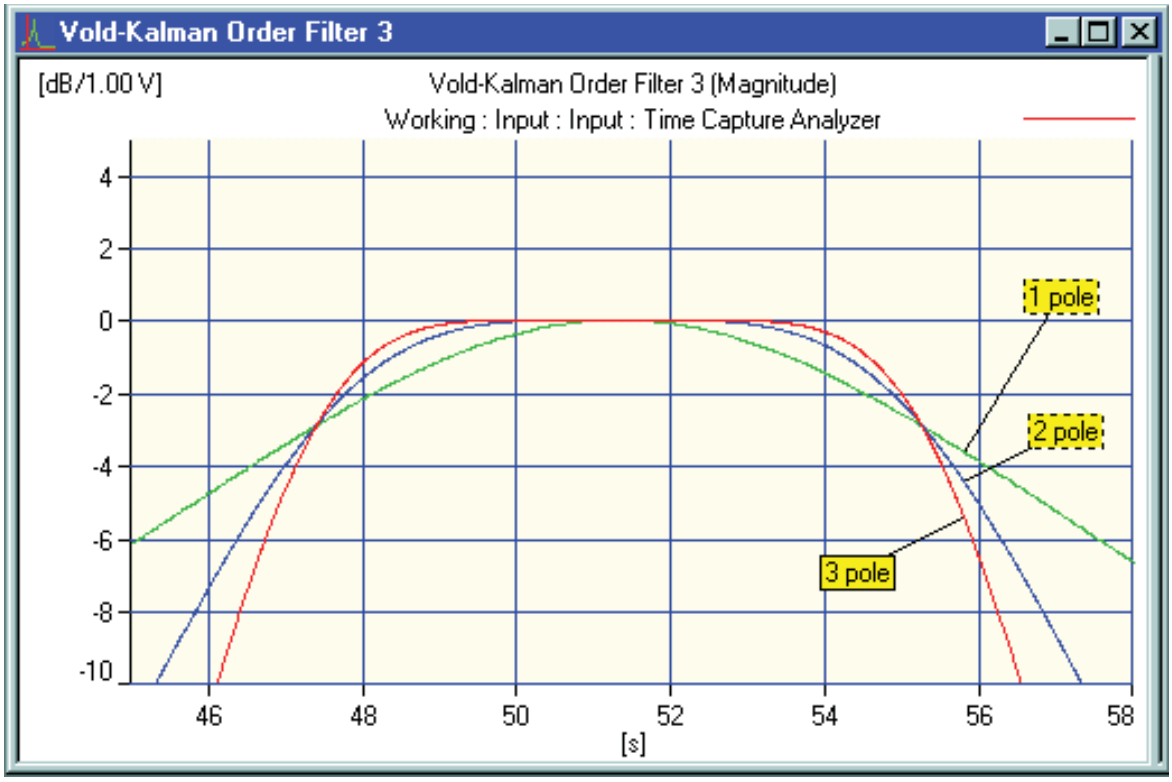

Fig. 20. Comparison of the frequency response in the passband for one-, two- and three-pole Vold-Kalman filters with the same bandwidth of 8 Hz

Another characteristic of the filter is the frequency response within the passband. As seen in Fig. 20 the two- and three-pole filters have a much flatter frequency response in the passband compared to the one-pole filter, with the three-pole filter having the flattest frequency response. The flatness of the frequency response in the passband is important when analyzing the amplitude and phase modulation of the harmonic carrier frequency. Amplitude and phase modulation corresponds in the frequency domain to sidebands centered around the harmonic carrier frequency component, which means that the more flat the frequency response is the more correct the modulation will show up the filter analysis.

The phase of the Frequency Responses for the different filter types is zero in the full frequency range within the measurable dynamic range. Thus there is no phase distortion or time delay for tracked orders including modulations identified as lower and upper sidebands.

Filter Characteristics in Time Domain

The time response of Vold-Kalman filters is important to understand when analyzing transient phenomena and responses to lightly damped resonances being excited during a run-up or a run-down. The time response has been investigated by applying a tone burst with a certain duration to a Vold-Kalman filter with a fixed centre frequency corresponding to the frequency of the toneburst. In Fig. 21 the magnitude (envelope) of the response of a filter centered at 100 Hz with a bandwidth of 8 Hz is shown using a logarithmic y-axis. A 100 Hz tone burst with a duration of 1 s is applied to the filter. One very important feature is that the time response is symmetrical in time, i.e. it appears to behave like a non-causal filter. This is because Vold-Kalman filtering is implemented as post processing allowing for non-causal filter implementation and extraction of order waveforms with no phase bias or distortion, i.e. without a time delay. Fig. 21 shows the time response for one-, two- and three-pole filters with a bandwidth of 8 Hz.

The one-pole filter has, as expected, the shortest decay time and an exponential decay which appears as a straight line when displayed with a logarithmic y-axis, while the two-pole and three-pole filters in addition to the longer

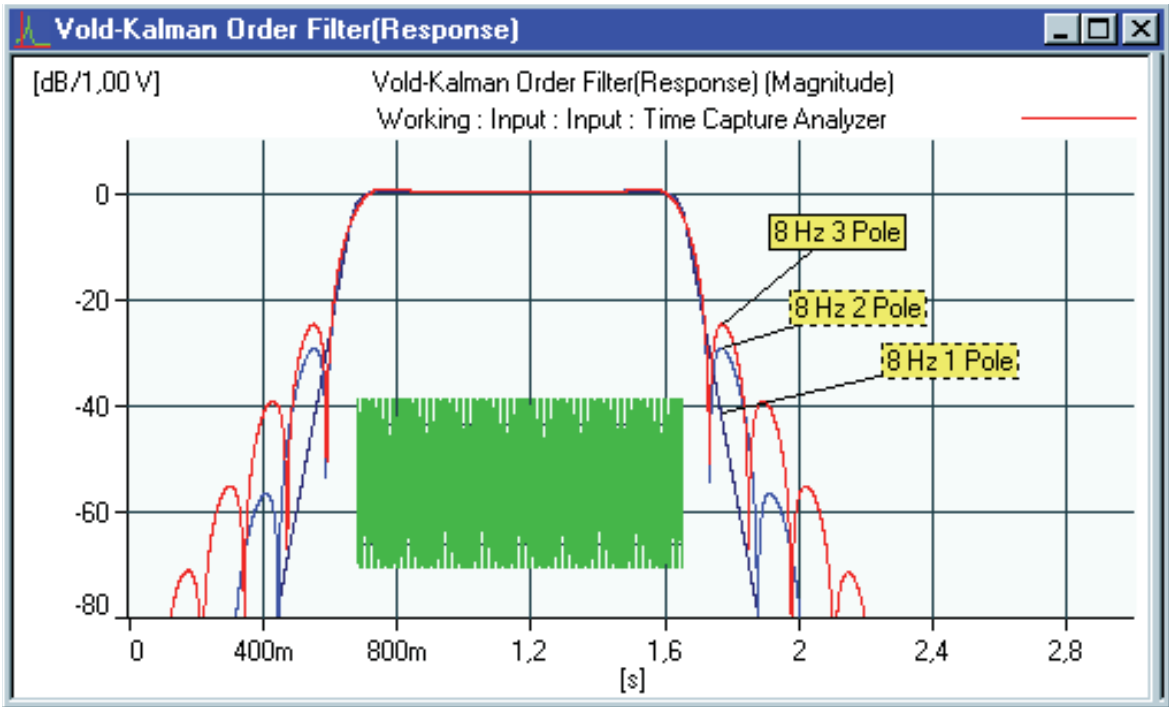

Fig. 21. Comparison of the magnitude of the time responses for one-, two- and three-pole Vold-Kalman filters with a bandwidth of 8 Hz. The applied signal, a tone burst of 1 s duration, is shown as well

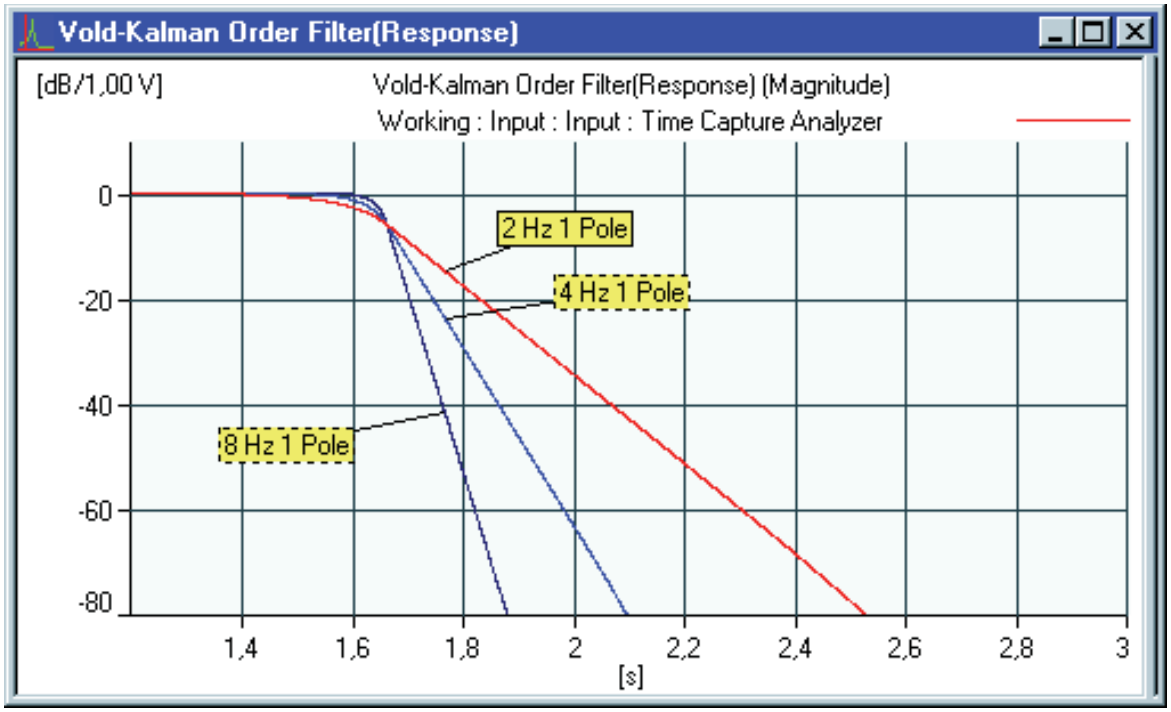

Fig. 22. Comparison of Time Responses for one-pole 2 Hz, 4 Hz and 8 Hz bandwidth Vold-Kalman filters. The applied signal is a tone burst of 1 s duration

decay times also show some lobes. The main lobes of all three filter types show on the other hand nearly the same progress in the upper 25 dB, i.e. the same "early decay", which means their behaviour in terms of how fast they can follow amplitude changes of orders are nearly identical.

Fig. 22 shows the time response of a one-pole filter for 3 different choices of filter bandwidths. As expected the decay time is inversely proportional to the bandwidth. Since the slope for a one-pole filter is very similar to the slope of the early decay for two- and three-pole filters with the same bandwidth we can extract the following important time-frequency relationship for all three types of Vold-Kalman filters,

$$B_{3dB} \times \tau = 0.2 \tag{9}$$

where B_{3dB} is the 3 dB bandwidth of the Vold-Kalman filter and τ is the time it takes for the time response to decay 8.69 dB ($= 10 \times \log e^2$). One pole filter is based on a second order structural equation, i.e. a one degree of freedom resonator (an SDOF system) which has the time-frequency relationship, $\sigma \times \tau = 1$ (see Ref. [19]) corresponding to $B_{3dB} \times \tau = 1/\pi$. Thus we have an optimum time-

frequency relationship close to the Heisenberg's uncertainty limit using Vold-Kalman filtering. Due to its symmetry the efficient duration of the time response has to be considered 2τ rather than τ. If reverberation time T_{60} instead of time constant τ is preferred, the relation (9) becomes,

$$B_{3dB} \times T_{60} = 1.4 \tag{10}$$

When zooming in around the beginning or the end of the tone burst a difference between the three filter types is revealed as seen in Fig. 23. The one-pole filter has a smooth decay before the stop of the tone burst, whereas the two-pole and the three-pole filters show a ripple with a maximum deviation (overshoot) from the steady state response of 0.28 dB and 0.46 dB respectively. This overshoot phenomenon is only seen in analysis results when analyzing signals with abrupt amplitude changes (such as in the case of a tone burst) or when a too narrow filter bandwidth is selected for the analysis (i.e., the time constant, τ of the filter is too long for the signal to be analyzed).

As an additional observation, all time responses have decayed to −6 dB, irrespective of the chosen filter parameters, at the location where the tone burst stops,

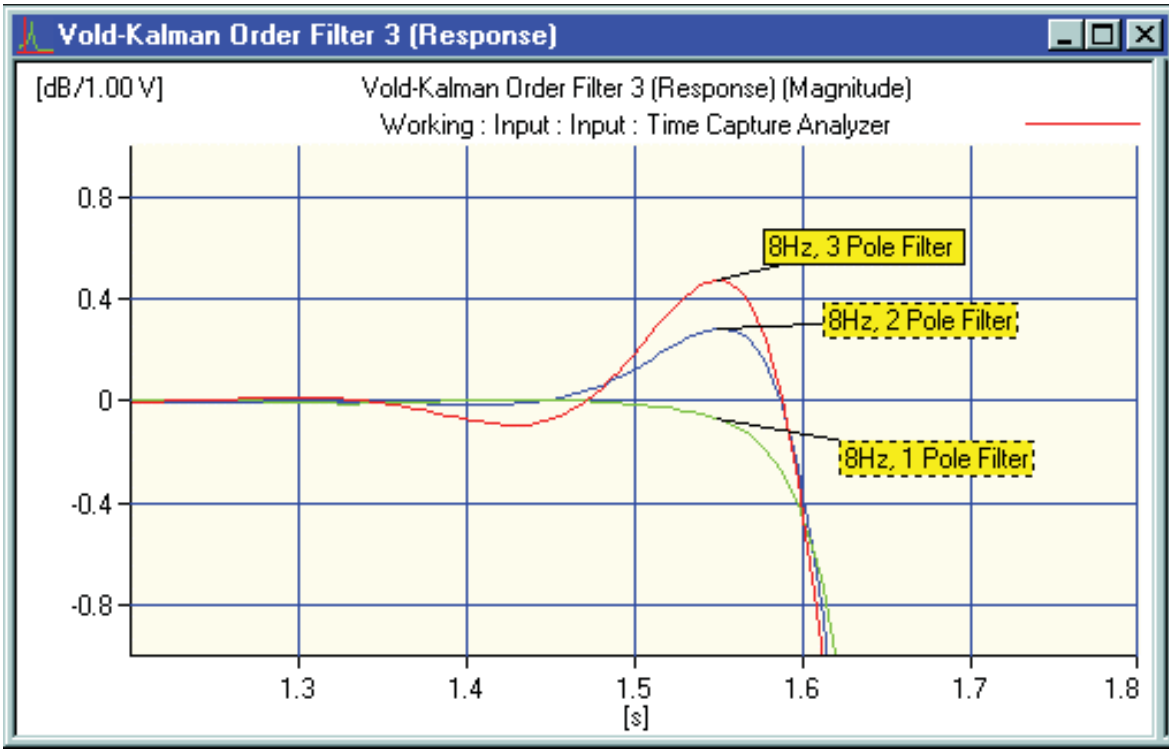

Fig. 23. Detailed picture of the time response of the one-, two- and three-pole filters at the end of the tone burst

see Figs. 21 and 22. (i.e. where the energy of the order signal inside the analyzed time window is reduced by 3 dB). Due to the sudden change in the nature of the signal, from a sine wave to nothing, a further leakage of the order, into neighbouring frequencies by 3 dB is seen. A similar effect is observed using FFT analysis. See Appendix A fore more details.

The phase curve is zero degrees in the full time range where the time burst exists as expected, except for some small edge effects (less than 1 degree for the 8 Hz fillter) at the two discontinuities, i.e., the Vold-Kalman filter has no time delay for a tracked signal.

Phase of Orders and Waveforms

The major question is: What is the reference for the detected phase? For the Phase Assigned Autospectrum in PULSE, the phase spectrum assigned to the autospectrum is the phase of the cross-spectrum between the selected signal and the reference signal selected by the user, e.g. a tacho signal or any other suitable signal. This is a typical dual channel measurement.

For the Vold-Kalman filtering the situation is slightly different, the phase is extracted from the vibration/acoustic signal itself, i.e. from one signal only:

In a time domain model the Vold-Kalman filter fits sine waves at the selected order/carrier frequency to the vibration/acoustic signal. For a one-pole filter three data samples are fitted at a time in a recursive manner [2, 20]. For two and three pole filters more samples are used in the curve fit/ filtering process.

The phase of a particular Phase Assigned Order component at time zero (beginning of time record) will be the phase at time zero for the curve fitted sine wave result, similar to the phase of a sine wave component in a Fourier Spectrum which is the phase of this component at the beginning of the time record. The standard convention is as follows: if a sine wave has its maximum amplitude at time zero, then the phase of its Fourier component is per definition 0 degrees. If a sine wave has its minimum amplitude at time zero, then the phase is 180 degrees. For zero crossings with positive and negative slopes the phase is minus 90 and plus 90 degrees respectively. Thus the starting phase for a Phase Assigned Order is the phase of the order signal itself irrespective of the actual starting phase of the tacho reference / carrier / RPM signal. This is also a consequence of the fact that only the RPM profile (i.e., frequency) and not phase is derived from the tacho signal. The phase of the tacho reference/carrier/RPM signal can then be regarded to have zero phase at time zero for any order of interest, and the phase for any order is thus assigned to the phase of the rotat-

ing shaft, i.e. the tacho signal with an arbitrary offset. The phase at any later time for the Phase Assigned Orders depends on the transfer properties between the forcing functions from the rotating shaft to the measurement/ observation position.

When calculating the order waveform from the Phase Assigned Orders and the RPM, the order waveform will have a phase at time zero which is the combination of the phase of the carrier wave (per definition 0 degrees) and the phase of the phase assigned order at time zero, which is the measured phase of the order waveform at time zero. Thus the output order waveform will have no phase shift, i.e. no time delay, with respect to the measured signal and thus can be used in synthesis studies as shown later.

Selection of Bandwidth and Filter Type

Selection of the filter bandwidth is basically a compromise between having a bandwidth which is sufficiently narrow to separate the various order components in the signal and a bandwidth which is sufficiently wide, i.e. giving a sufficiently short filter response time, in order to follow the changes in the signal amplitude. The contour plot of the STFT analysis can be used for evaluating the separation of the various components. Using the radio signal analogy this means that not only the carrier frequency located at the centre frequency of the filter, but also the AM/FM modulation components should be inside the filter passband, since it is these components that contain the information of interest. An extremely narrow filter that suppresses all the sidebands would produce an order with constant magnitude as a function of time and constant slope of the phase.

Various research tests have shown that when orders pass through a resonance the time constant of the filter, τ, should be shorter than 1/10 of the time, T_{3dB} , it takes for the particular order to sweep through the 3 dB bandwidth of the resonance, Δf_{3dB}. This ensures an error of less than 0.5 dB of the peak amplitude at the resonance using a one-pole filter. For two- and three-pole filters the error of the measured peak will be less. If no resonance is observed in the extracted orders the (minimum) time it takes for the order to increase/ decrease 6 dB may be used instead.

Thus for the time constant of the filter we have that:

$$\tau \leq (1/10) \times T_{3dB} \tag{11}$$

or when combining (9) and (11) in terms of the bandwidth of the filter:

$$B_{3dB} = 0.2/\tau \geq 2/T_{3dB} \quad (12)$$

The time it takes for order number k to sweep through the 3dB bandwidth is

$$T_{3dB} = \Delta f_{3dB}/(k \times SR_{Hz}) \quad (13)$$

or

$$T_{3dB} = \Delta f_{3dB}/(k \times SR_{RPM}/60) \quad (14)$$

where SR_{Hz} and SR_{RPM} is the sweep rate in Hz/s and RPM/s, respectively. This means that the bandwidth, B_{3dB} of the Vold-Kalman filter extracting order number k should follow,

$$B_{3dB} \geq (2 \times k \times SR_{Hz})/\Delta f_{3dB} \quad (15)$$

or

$$B_{3dB} \geq (k \times SR_{RPM})/(30 \times \Delta f_{3dB}) \quad (16)$$

i.e. the selected bandwidth should be chosen so that it is proportional to the order number and the sweep rate, and inversely proportional to the bandwidth of the resonance of interest.

When the sweep rate and bandwidth in (16) are unknown, it is more practical to use equation (12) as shown in example 2.

Example 1

In the first example a linear sweep of a square wave, with a sweep rate of 17200 RPM/s from 12000 RPM to 63000 RPM (286.7 Hz/s from 200 Hz to 1050 Hz), passing through a known resonance is analyzed. The resonance frequency is 795 Hz and the 3 dB bandwidth of the resonance is 16 Hz, corresponding to 1% damping. The first three orders are analyzed. Using (16) we have for the 1st order:

$$B_{3dB} \geq (1 \times 17200)/(30 \times 16)\,\text{Hz} = 35.8\,\text{Hz}$$

for the 2nd order:

$$B_{3dB} \geq (2 \times 17200) / (30 \times 16)\,\text{Hz} = 71.6\,\text{Hz}$$

and for the 3rd order:

$$B_{3dB} \geq (3 \times 17200) / (30 \times 16)\,\text{Hz} = 107.5\,\text{Hz}$$

The Vold-Kalman filter bandwidth can be specified in terms of constant frequency bandwidth or proportional to RPM bandwidth (i.e., constant percentage bandwidth). For proportional bandwidth the value is entered as a percentage of the basic shaft speed, thus 10% bandwidth gives a resolution of 0.1 order. Proportional bandwidth is the best choice when analyzing over wide RPM ranges or when analyzing higher orders. A bandwidth of 35.8 Hz for the 1st order at the resonance frequency of 795 Hz corresponds to 4.5% bandwidth, a bandwidth of 71.6 Hz for the 2nd order at 795 Hz corresponds to 18% bandwidth and a bandwidth of 107.5 Hz for the 3rd order at 795 Hz corresponds to 40% bandwidth. Fig. 24 shows the magnitude of the Phase Assigned Orders extracted with a two-pole filter with proportional bandwidth of 4.5%, 18% and 40% for the 1st, 2nd and 3rd orders respectively.

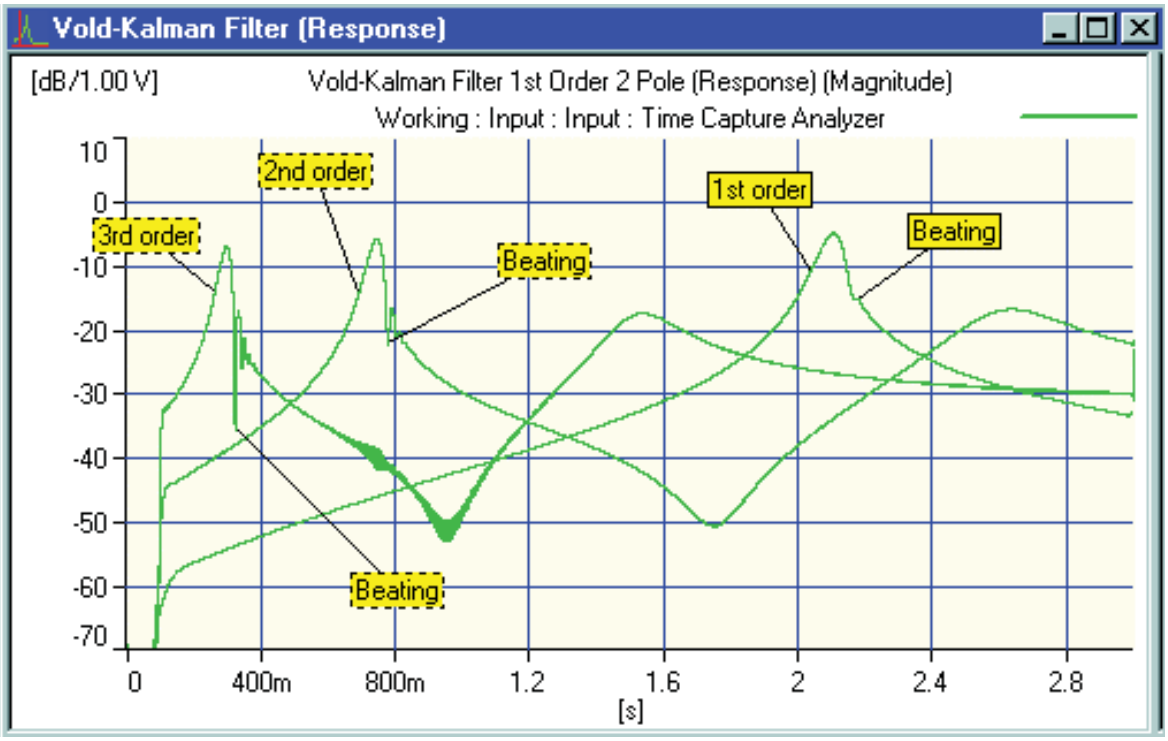

Fig. 24. Magnitude of the Phase Assigned Orders of the first three orders extracted with a two-pole Vold-Kalman filter with bandwidths of 4.5%, 18% and 40% respectively

The peak amplitudes measured with one-, two- and three-pole filters with bandwidths of 4.5%, 18% and 40% for the 1st, 2nd and the 3rd orders respectively are given in Table 1. The correct peak amplitudes were found by widening the filter bandwidth until the amplitude did not increase any more.

Table of measured peak amplitudes	One-pole filter 4.5%, 18%, 40%	Two-pole filter 4.5%, 18%, 40%	Three-pole filter 4.5%,18%, 40%	Correct Amplitude
1st order	–5.3 dB	–5.1 dB	–5.0 dB	–5.0 dB
2nd order	–6.3 dB	–6.0 dB	–6.0 dB	–6.0 dB
3rd order	–7.4 dB	–7.2 dB	–7.1 dB	–7.1 dB

Table 1. Peak amplitudes in dB for the 1st, 2nd and 3rd order component extracted with one-, two-, and three-pole Vold-Kalman filters with bandwidths of 4.5%, 18% and 40% respectively

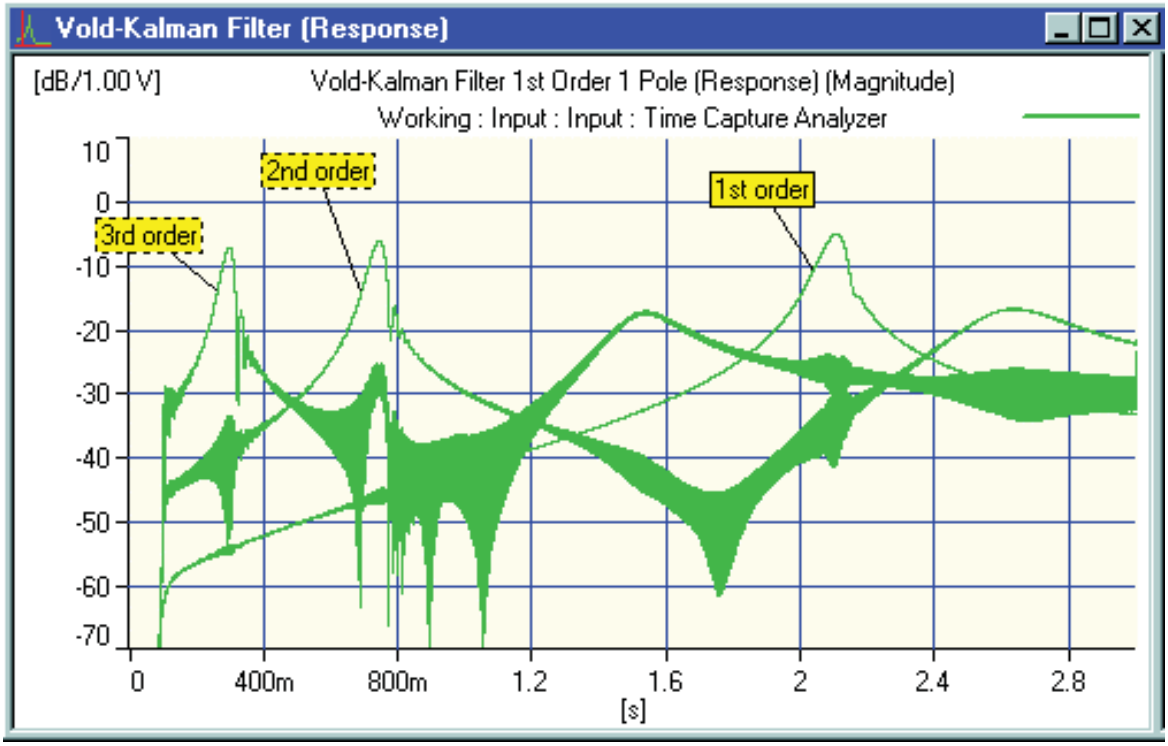

Fig. 25. Magnitude of the Phase Assigned Orders of the first three orders extracted with a one-pole Vold-Kalman filter with bandwidths of 4.5%, 18% and 40% respectively. Notice the interference due to the limited selectivity of the one-pole filter

The peak amplitude errors for the one-pole filter is thus 0.3 dB and for the two- and three-pole filters within 0.1 dB having a minimum bandwidth given by (16).

A second resonance at 1900 Hz, being excited by the second and the third orders, is also seen in Fig. 24.

Using a filter with proper selectivity is very important for the analysis. This is illustrated in Fig. 25, which shows the result of the Vold-Kalman filtering using the one-pole filter instead of the two-pole filter used in Fig. 24. All other analysis parameters are kept unchanged. The limited selectivity of the one-pole filter causes a lot of interference from the other orders especially at the positions where these pass through the resonances. The interference is most dominant for the 3rd order due to the wider bandwidth needed to extract this order. The interference from the 2nd order can even lead to misinterpretations of "non-existing" resonances. Decoupling cannot be used to avoid this kind of interference over a wide time span. Using the two-pole filter (Fig. 24) a small amount of interference is still seen for the 3rd order in the analysis. The three-pole filter will completely suppress the interference from the other orders in this case.

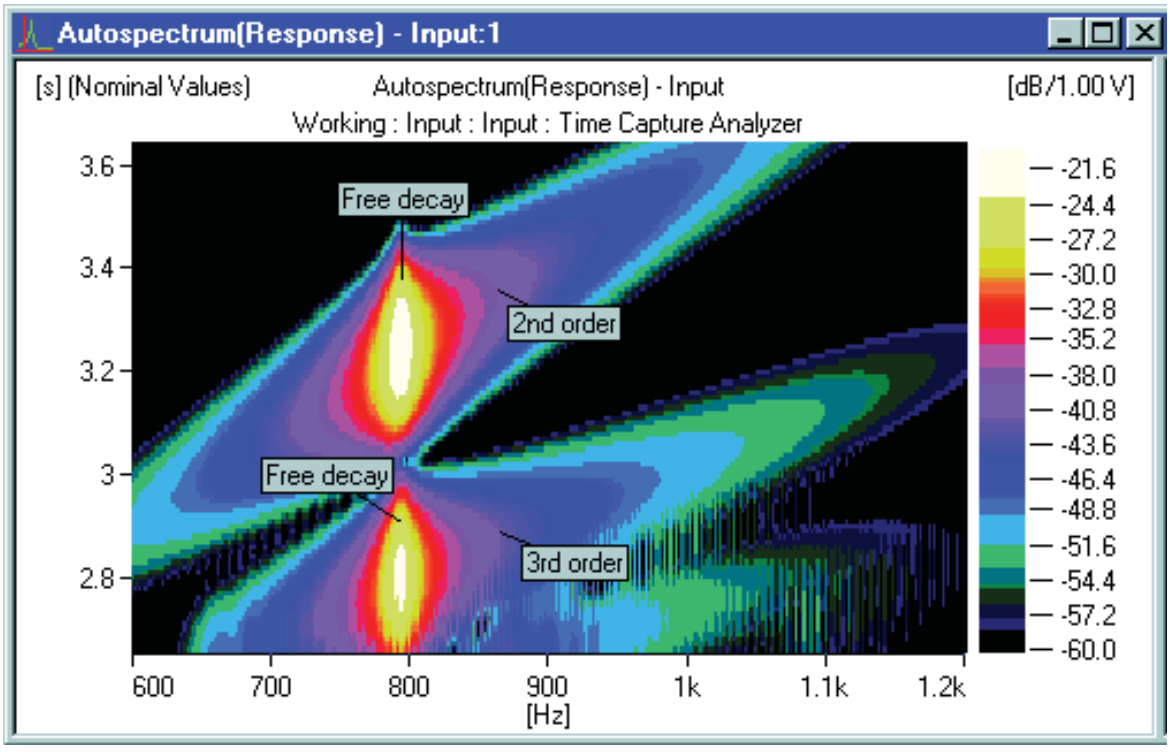

Fig. 26. Detailed view of the part in the contour plot where the 2nd and 3rd order components excite the first resonance. The free decay of the damped natural frequency of 795 Hz is clearly seen. A 3200 line analysis, giving Δf of 2 Hz, and a step of 10 ms between the spectra is used

The ripples indicated in Fig. 24, on the decaying slope after the orders have passed the resonance still need some explanation. These ripples are caused by an interaction between the order component and the free decay of the natural frequency for the lightly damped resonance. This phenomenon can be investigated by looking at the contour plot of an STFT analysis. Fig. 26 shows a detailed view of the part in the contour plot where the 2nd and 3rd order components excite the first resonance. A 3200 line analysis, giving a Δf of 2 Hz, and a step of 10 ms between the spectra (corresponding to 98% overlap) is used. The free decay of the resonance after the point in time where the orders have "crossed" the resonance frequency is clearly seen. When the decaying oscillations of the damped natural frequency are inside the passband of the filter extracting the given order, the beating interference will occur. The beating is most severe for the third order because of the wider bandwidth used in the analysis. Since there is no "natural" tacho signal, which relates to the damped natural frequency, it is not possible to make decoupling of these components.

The only way to get less beating interaction is to use a narrower filter bandwidth in order to get the free decaying natural frequency faster outside the passband bandwidth after the resonance crossing of the order. This will, however, cause violation on the requirement of the minimum bandwidth given by (12), (15) or (16).

Example 2

In this example a fast run-up of a spin - drier is analyzed. A tacho signal giving 12 pulses per revolution is used and the vibration responses in the tangential, radial and axial directions are measured. Fig. 27 shows the contour plot of the STFT analysis of the radial response. It is seen that the response is dominated by the 1st order (unbalance) and the 22nd order. Each Fourier transform is based upon a record length of 250 ms giving a line spacing Δf of 4 Hz.

The 1st order is dominated by one resonance. The run-up takes approximately 6 seconds and the curve fitted RPM profile is shown in Fig. 28.

The peak value and the time, $T_{3\,dB}$ it takes for the 1st order to sweep through the 3 dB bandwidth of the dominating resonance is found by applying a three-pole filter with wide bandwidth (up to 100%). Using a bandwidth of more than 100% gives ripples due to beating interference even with the three-pole filter. From these analyses $T_{3\,dB}$ is found to be 464 ms and the peak of the resonance is found to be 12.6 dB. Using (12) this means that the minimum bandwidth should be 4.31 Hz. The peak of the resonance is at 681 RPM (11.3 Hz) which means that the minimum bandwidth should be 38%. Using a bandwidth of 38% gives a peak value of 12.2 dB (i.e., an error of 0.4 dB).

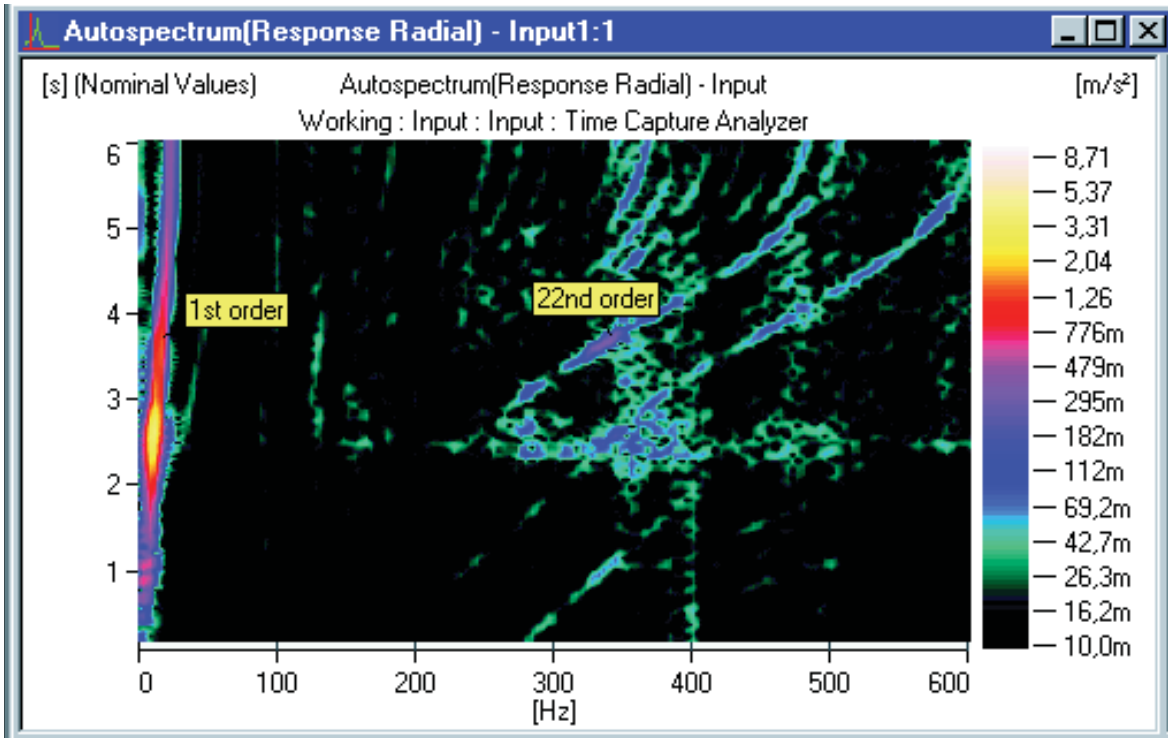

Fig. 27. Contour plot of an STFT analysis of a run-up of a spin drier

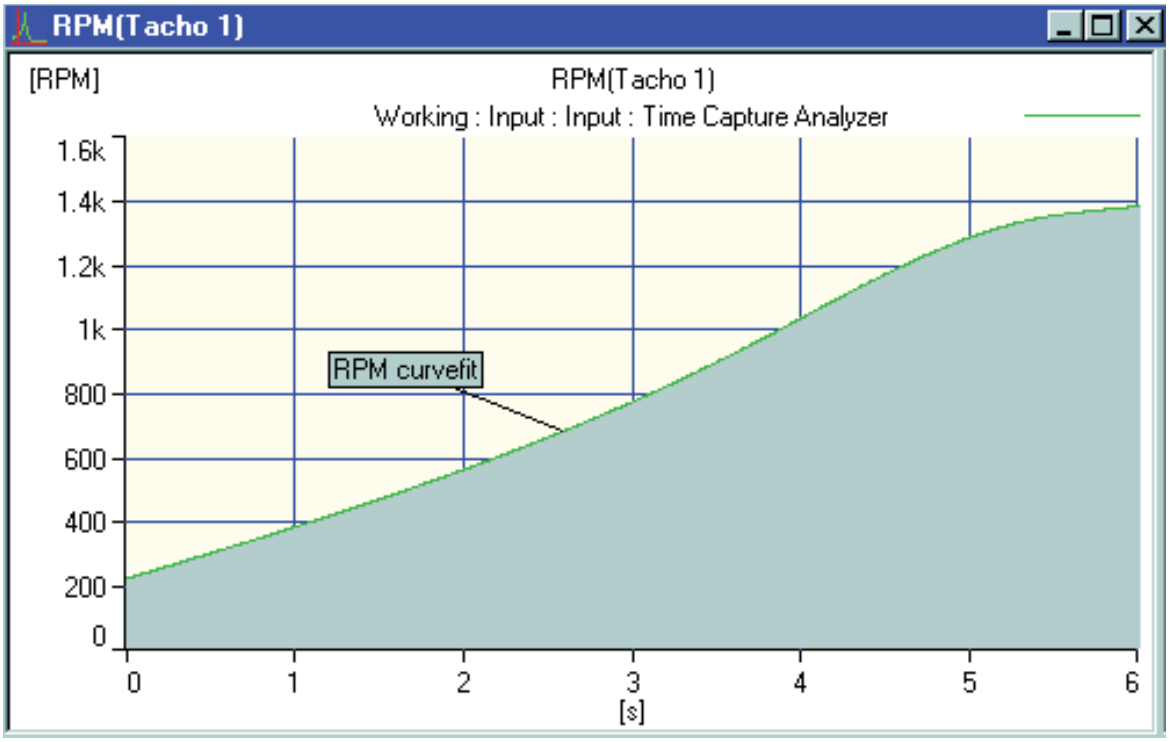

Fig. 28. Curve-fit of RPM as a function of time used as input for Vold-Kalman filtering

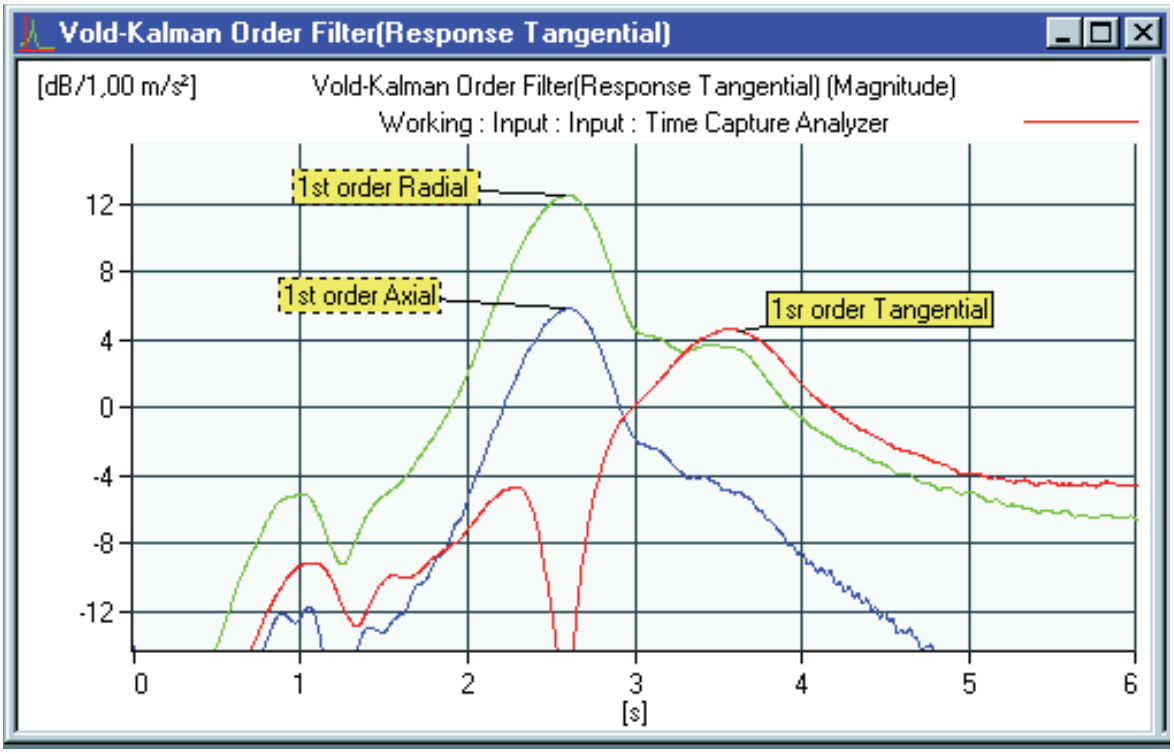

Fig. 29. 1st order of the radial, tangential and axial response, during a run-up of the spin drier, extracted using a three-pole Vold-Kalman filter with 50% bandwidth

The same peak value is found using one-pole and two-pole filters. For the one-pole filter with 38% bandwidth the extracted order is, however, contaminated by ripples (beating interference), even at the resonance, due to the limited selectivity. Fig. 29 shows the 1st order of the radial, tangential and axial response extracted using a three-pole filter with a bandwidth of 50%. The same resonance is seen in the axial response, whereas the dominating resonance in the tangential response is at 911 RPM (15.2 Hz). A lower resonance at 375 RPM (6.25 Hz) is seen in the radial and axial response and at 388 RPM (6.47 Hz) in the tangential response. $T_{3\,dB}$ for this resonance is found to be 415 ms for the radial response indicating that the bandwidth should be at least 76%. Using 50% bandwidth with a three-pole filter gives an under-estimation of approximately 0.8 dB. A two-pole filter gives a beating interference at this resonance with bandwidth larger than 50%, and proper measurement of this resonance is not possible with a one-pole filter due to strong beating interference even for bandwidth as narrow as 20%. The 22nd order can be extracted using a three-pole filter with a bandwidth of 60%, which is found to be the minimum bandwidth for the dominating

resonance at 933 RPM (15.6 Hz) in the radial response. A two-pole filter gives a small interference at the resonance with 60% bandwidth, and for a one-pole filter interference is experienced for bandwidths wider than 40%.

Crossing Orders

To illustrate the effectiveness of the Vold-Kalman filter with decoupling of close and crossing orders, two signals have been mixed, a 1 kHz signal and a 300 Hz to 2000 Hz swept signal containing several orders as shown in the STFT contour plot in Fig. 30. The duration of the signal is 6 s. The example simulates a system with two independent axles. All orders and the 1 kHz sine wave were generated with constant amplitude.

The first two swept orders and the 1 kHz signal were extracted using 10% bandwidth (0.1 order resolution) two-pole Vold-Kalman filters without decoupling. The magnitude of the two swept orders is shown in Fig. 31 and the 1 kHz signal is shown in Fig. 32. As seen in this case the 1 kHz order strongly interacts with the swept 4th order around time 0.1 s, the 3rd order around time 0.4 s,

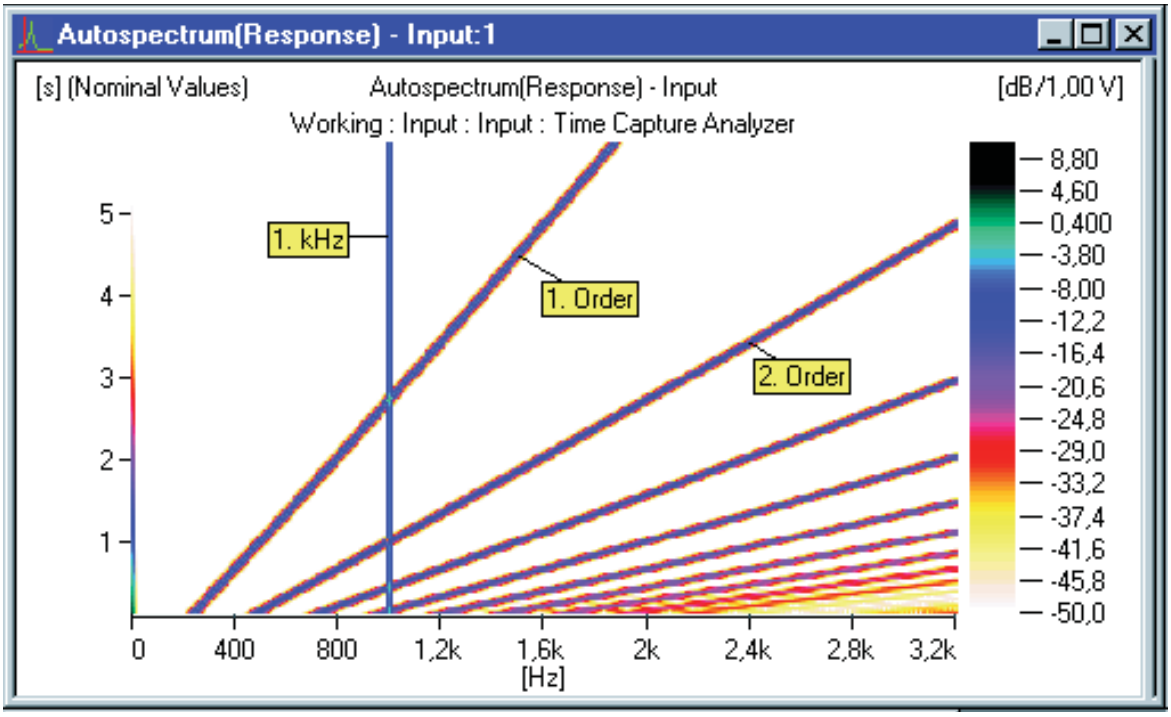

Fig. 30. An STFT of a signal mixed from a 1 kHz sine wave and a swept signal containing several harmonics (orders)

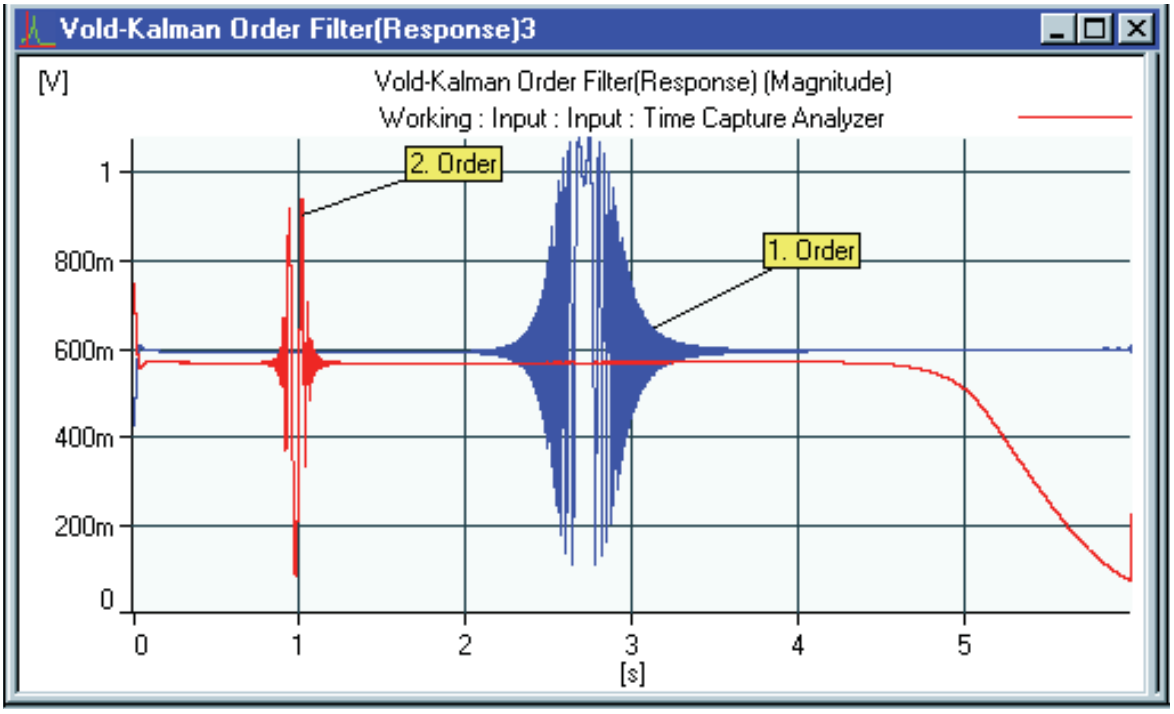

Fig. 31. First and second order of the swept signal extracted without decoupling using two-pole Vold-Kalman filter with a bandwidth of 10%

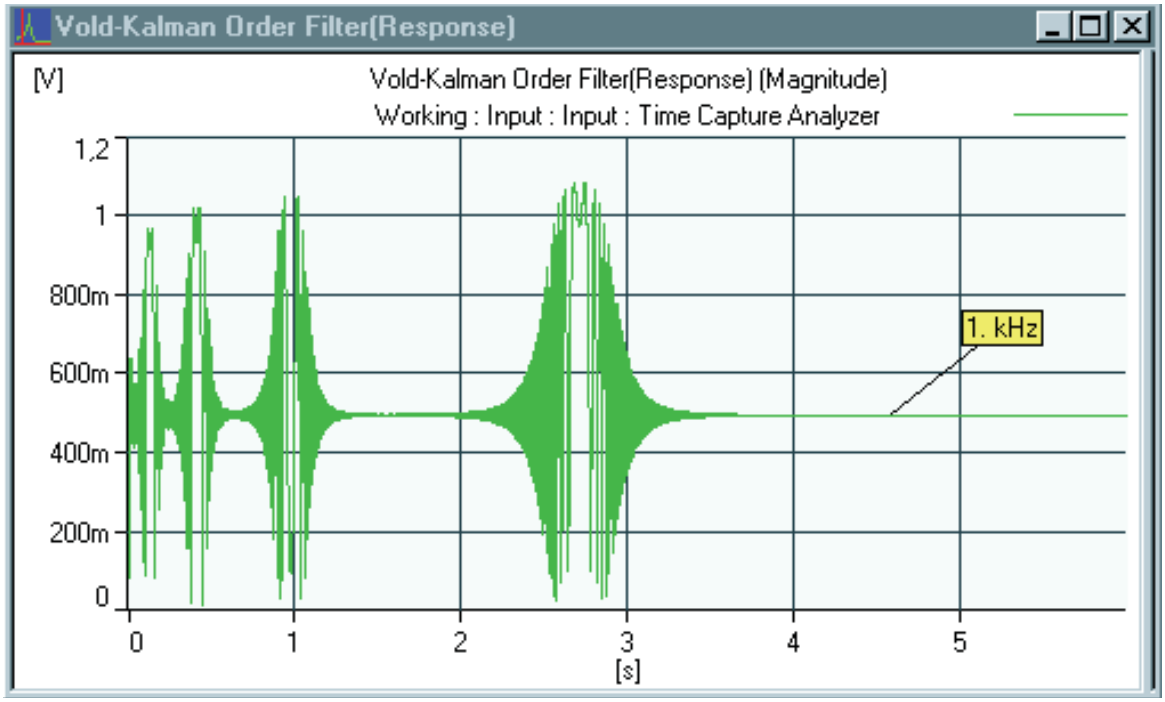

Fig. 32. 1 kHz signal extracted without decoupling using two-pole Vold-Kalman filter with a bandwidth of 10%

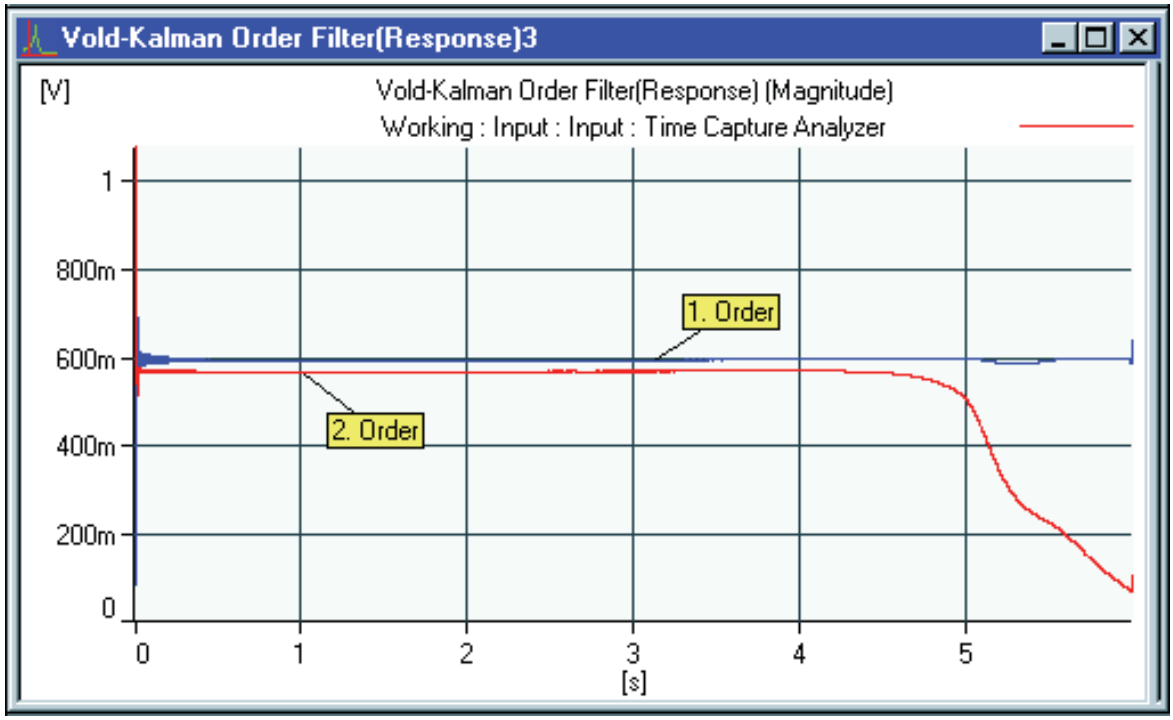

Fig. 33. First and second order of the swept signal extracted using decoupling and two-pole Vold-Kalman filter with a bandwidth of 10%

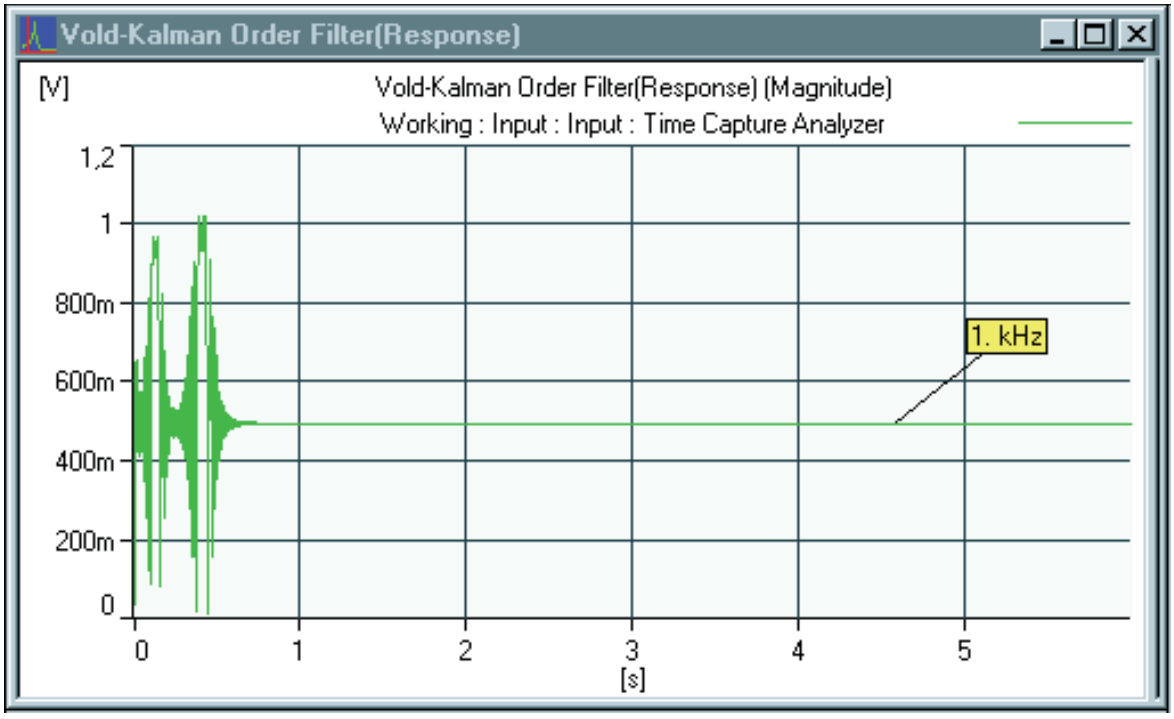

Fig. 34. 1 kHz signal extracted using decoupling and two-pole Vold-Kalman filter with a bandwidth of 10%

the 2nd order around time 1 s and the first order around time 2.7 s respectively, showing strong beating phenomena.

When the two tacho signals are used in a simultaneous estimation (i.e. with decoupling), but with the same filter parameters as in the single order estimation (i.e. without decoupling), we achieve a dramatic improvement in the quality of estimation, see Fig. 33 and Fig. 34. However, the 1 kHz still interacts with the swept orders nos. 3 & 4, since they were not included in the calculations.

Crossing orders from two independent motors

In this example the vibration response from two independent rotating motors is analysed. The response is measured at the support structure in a situation where one motor is running up and the other is running down resulting in crossing orders. In Fig. 35 the speed versus time functions (RPM profiles) of the two motors are shown.

The first order from the two motors is extracted using a two-pole Vold-Kalman filter with a bandwidth of 20%. The magnitude of the phase assigned orders is shown in Fig. 36.

A strong interaction between the two orders is seen in the area where the orders are crossing, i.e. where both orders are inside the filter passband.

Applying the decoupling technique with the filter setting otherwise unchanged the same two first order components are extracted as shown in Fig. 37.

In order to verify the fidelity of the decoupling technique an analysis of a run-up of motor 2, with motor 1 switched off, was performed. The magnitude of the first order of motor 2 from this test is shown as a function of time in Fig. 38. The same filter parameters as in the previous tests are used. The shape of the order is very similar to that calculated using decoupling shown in Fig. 37 verifying the validity of the decoupling technique. The acceleration of motor 2, in the case with motor 1 switched off, was a little lower compared to the case where both motors were running. The order, shown as a function of time, in Fig. 38 therefore seems stretched (delayed) compared to that shown in Fig. 37. This could also be one of the reasons why the peak amplitude of the dominating resonance (at 1.3 s and 1.4 s respectively) gets a little higher in Fig. 38. Another reason could be that the resonance is rather sensitive to boundary conditions and these might not be exactly the same in the two cases.

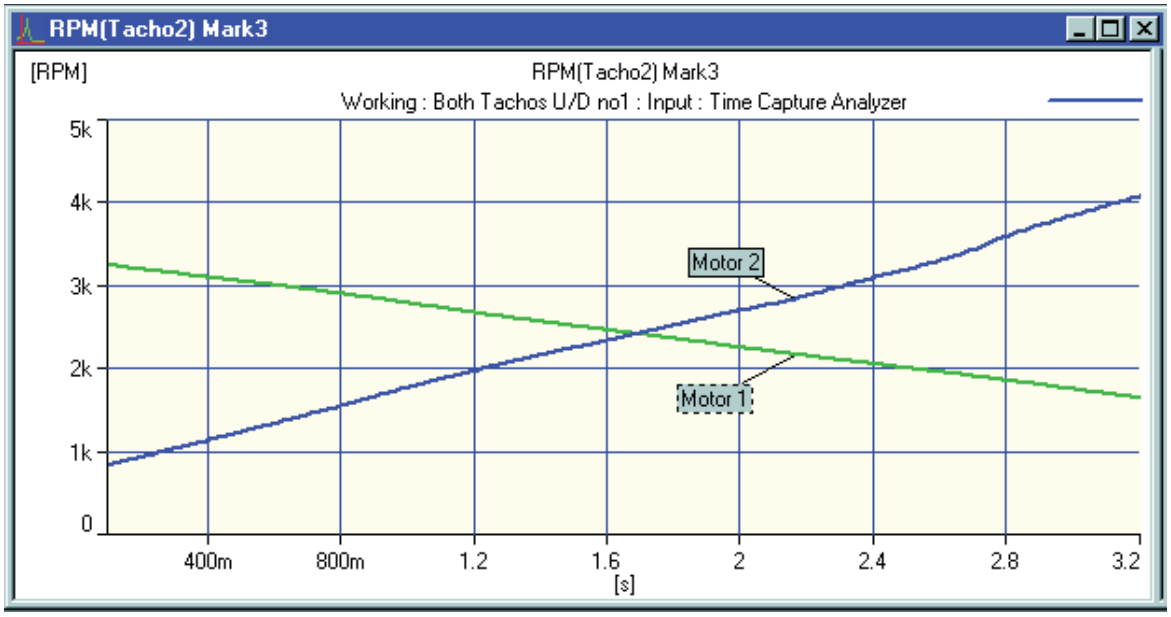

Fig. 35. RPM as a function of time (speed profile) for motor 1 (green) and motor 2 (blue)

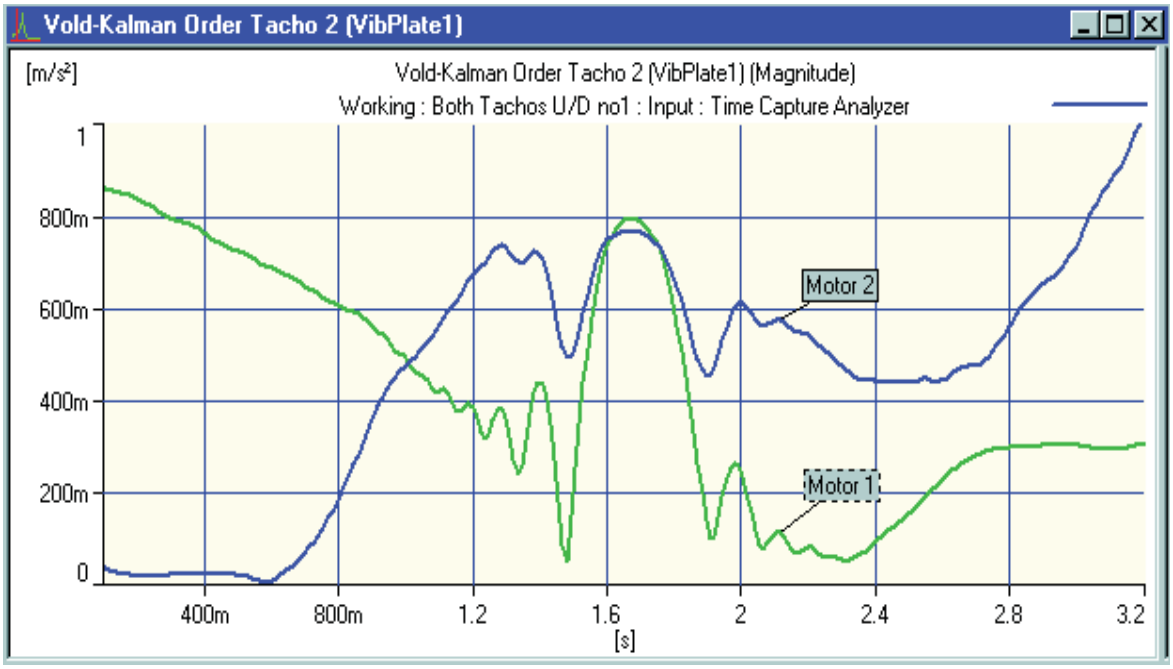

Fig. 36. First order of the two motors extracted using a two-pole Vold-Kalman filter with a bandwidth of 20%. Notice the strong interaction (beating) between the two orders in the area where the orders are crossing

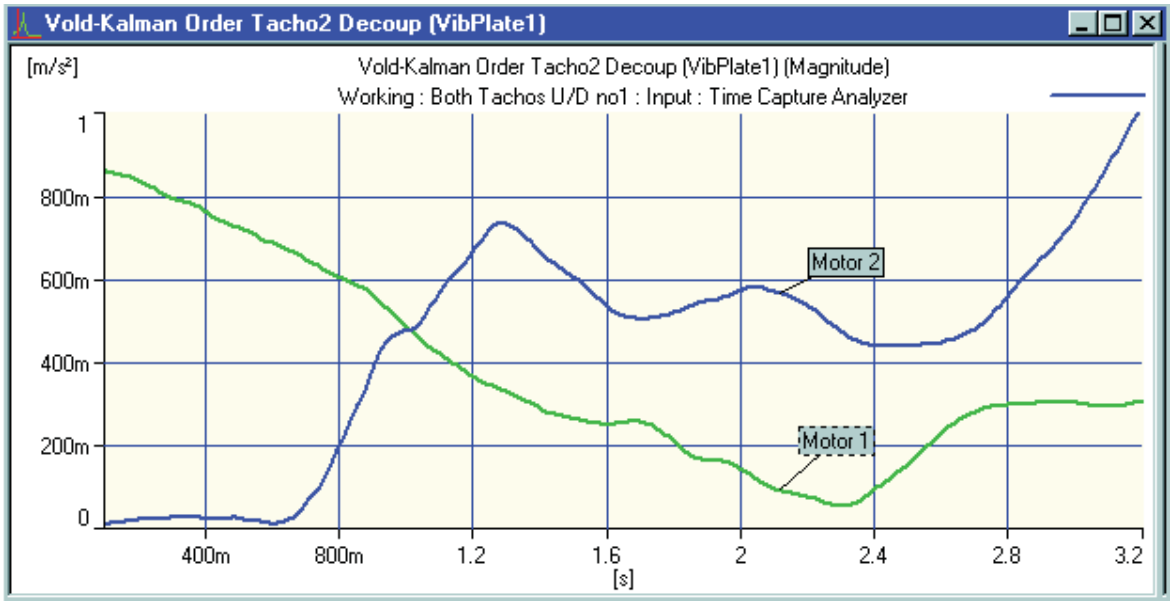

Fig. 37. First order of the two motors extracted using decoupling. Vold-Kalman filter setting otherwise as in Fig.36 without the decoupling. Notice that the interaction (beating) between the orders is avoided

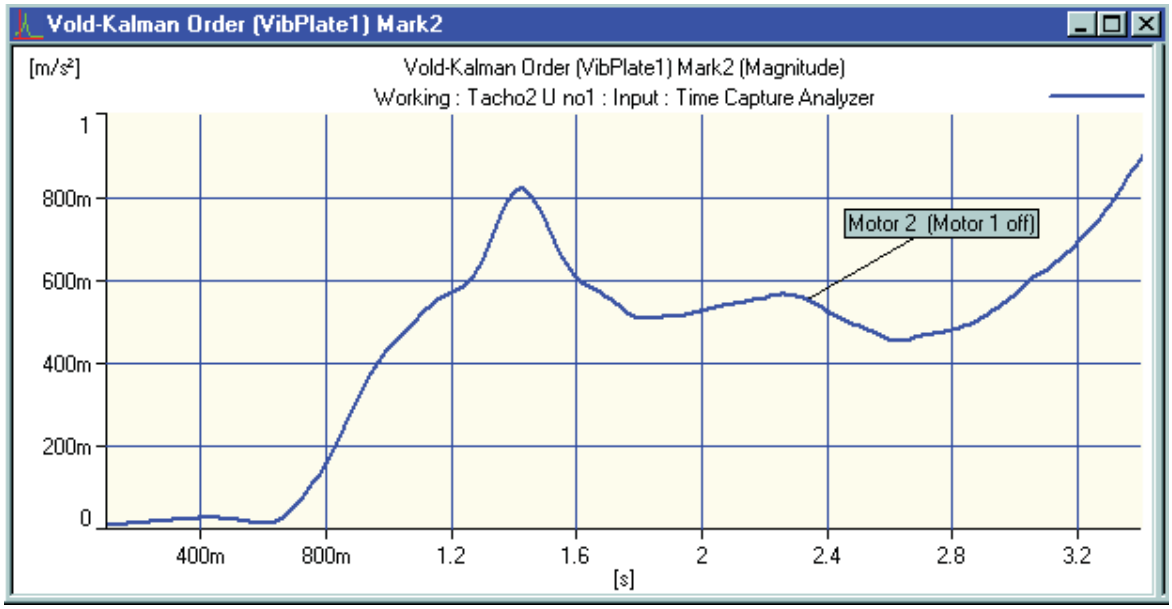

Fig. 38. First order in a run-up of motor 2 without motor 1 running. The Vold-Kalman filter parameters are the same as those used in Fig. 36 and Fig. 37. The result should be compared to that of motor 2 in Fig. 37 using decoupling

Sound Quality Synthesis

Since the Vold-Kalman filter extracts order waveforms without time delay, i.e., the extracted order time signals are coincident with the total signal; these time signals can be used for synthesis studies. This is especially interesting in the field of Sound Quality Engineering, where time-, frequency- and order-editing and simulation of acoustic signals is an important tool for product sound optimisation. In the following simple example the Brüel & Kjær Sound Quality Software Type 7698 has been used for post-processing of Vold-Kalman data. For sound perception the most dominating order is the 9th in the example shown in Figs. 10 – 17. The 9th order waveform was subtracted (any amount of attenuation is possible) from the total waveform using the mixer editing facility in version 3.0 of Type 7698 software. The time signal with the 9th order removed is shown in Fig. 39, but a comparison with Fig. 10 reveals no apparent visual difference, due to the fact that the amplitude of the 9th order (see Fig. 16) is about a factor of two smaller than the amplitude of the first order.

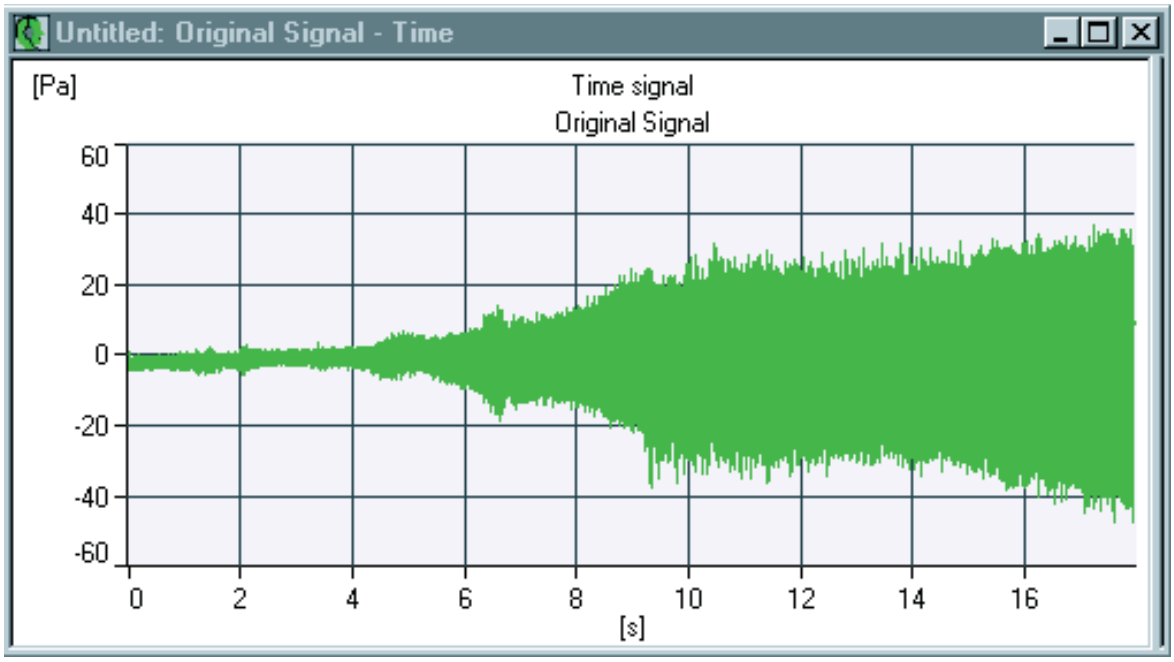

Fig. 39. Vibration time signal of the run-up with the 9th order removed (The amplitude scale changed to Pa)

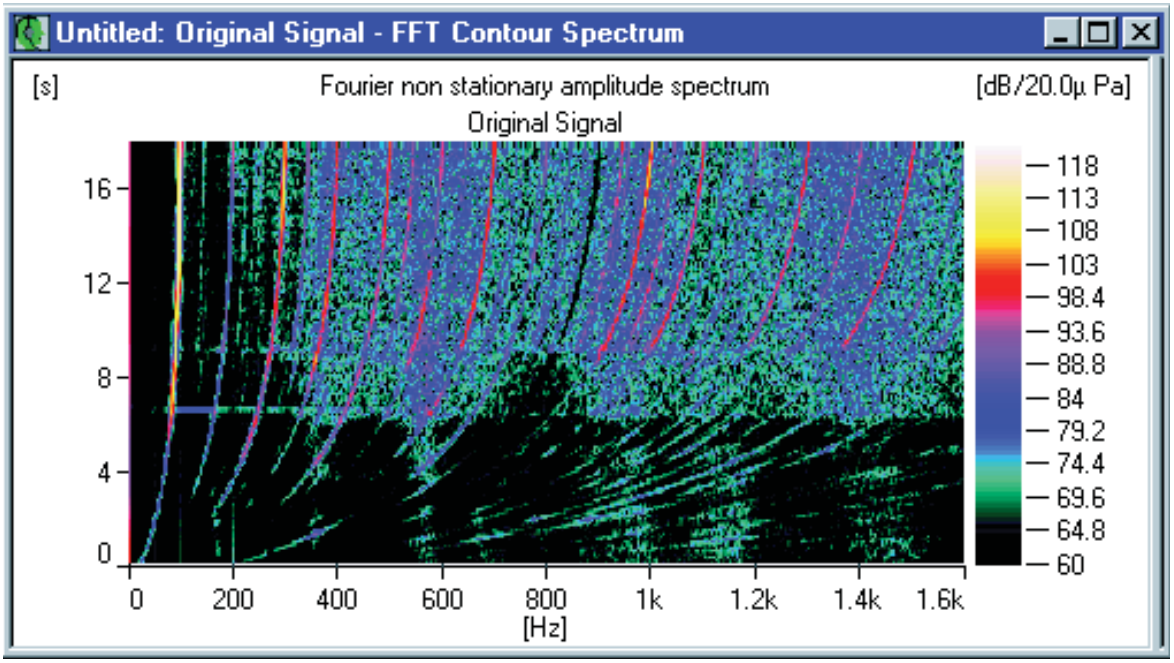

Fig. 40. An STFT of the vibration signal with the 9th order removed

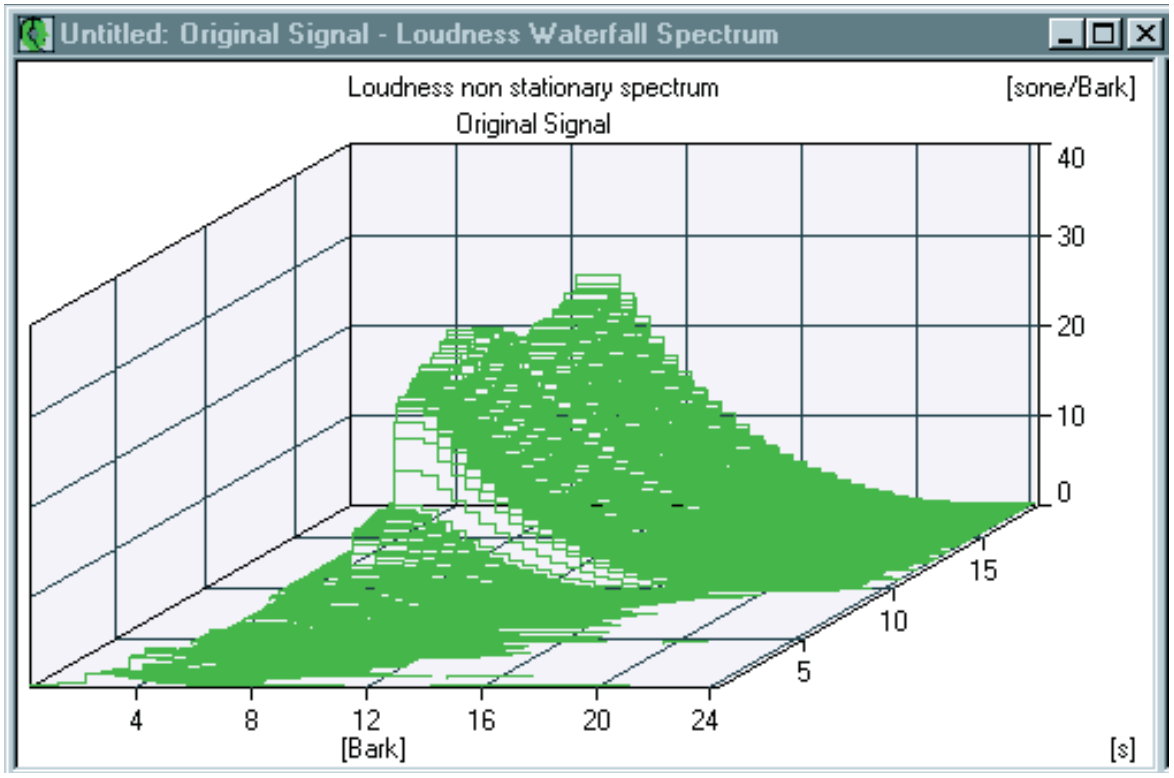

Fig. 41. Loudness analysis of the 9th order. Especially the frequency masking effect is clearly seen

It is on the other hand quite evident from the STFT contour plot shown in Fig. 40 compared to Fig. 11, that the 9th order has been removed as well as this was audible from a playback via the sound card of the original and edited signals. Since Type 7698 is a dedicated package for sound measurement, the amplitude scaling is in SPL or Pa rms amplitudes rather than vibration levels or vibration rms amplitudes. The SQ application provides the ability to listen to both the extracted orders and to the residual sound with the orders removed.

The individual orders may be analysed using STFT, digital filtering (using standardised filter shapes such as 1/3-octaves), Loudness Analysis or other techniques such as Wavelets or Wigner-Ville distribution [11, 21]. Fig. 41 shows an example where the 9th order waveform has been analysed using non-stationary Loudness calculations in order to study both time and frequency masking effects of the specific order.

Gearshift Example

The measurement was done on a light truck with a V-8 engine and an overdrive automatic transmission, which was run on a dynamometer in a semi-anechoic room. Data was acquired using an eight-channel DAT recorder and shown here calibrated in volts, i.e. uncalibrated with respect to engineering units, such as Pa and m/s^2. Using PULSE Interface to SONY DAT – Type 7706 the digital data was interpolated and resampled and directly analyzed by PULSE via a SONY PCIF 500 SCSI interface box without any need for further digital/analogue/digital conversions. For this example a full-throttle run-up was performed under light load condition, using a tractive (drag) force of only 50 lbf (≈222 N). Fig. 42 shows the RPM versus time curves from the tachometers on both the engine and the drive shaft (propeller shaft) for the complete run using a wide frequency and time range pre-analysis. See also Ref. [3] for more details.

Microphone signals from a binaural recording using a Brüel & Kjær HATS (Head and Torso Simulator) Type 4100 in the passenger seat, as well as accelerometer signals at several locations (pinion gear housing, transmission case at drive shaft side etc.), were recorded. The right ear signal from the HATS was analyzed in order to illustrate the capability of the Vold-Kalman Order Tracking Filter for handling gearshifts. It was decided to focus on the shift from the 2nd gear into the 3rd gear around time 11,5 s shown in Fig. 42. Thus a second PULSE multi-analysis of the recording was performed using a Tachometer Analyzer for triggering and RPM detection and monitoring purposes, an FFT analyzer for real-time FFT-order processing and a Time Capture Analyzer for capturing data for Vold-Kalman order tracking analysis.

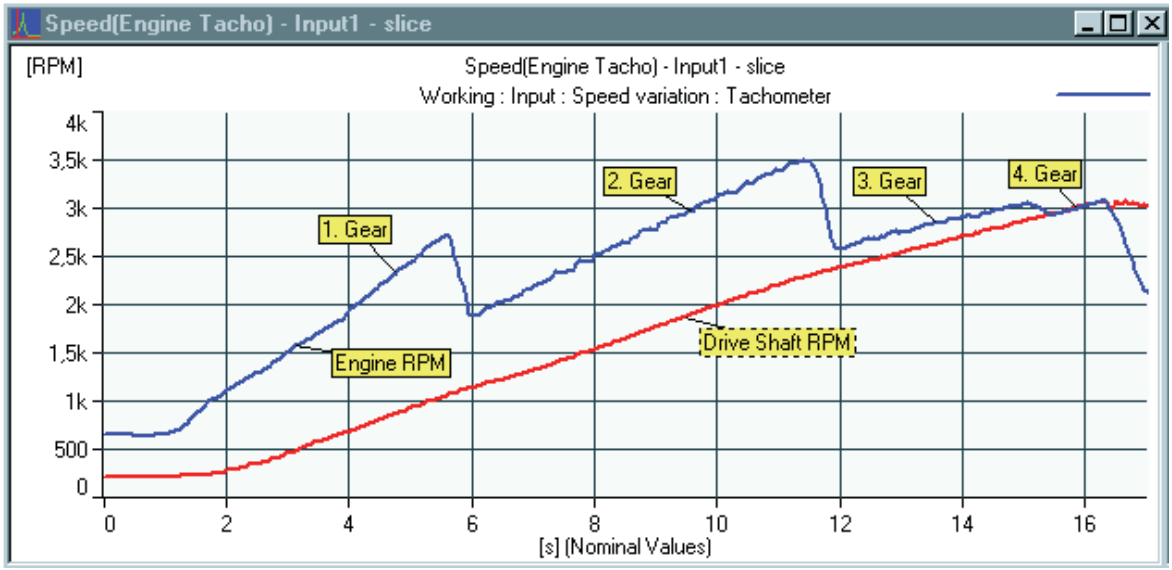

Fig. 42. RPM profiles of run-up, with gear shift events

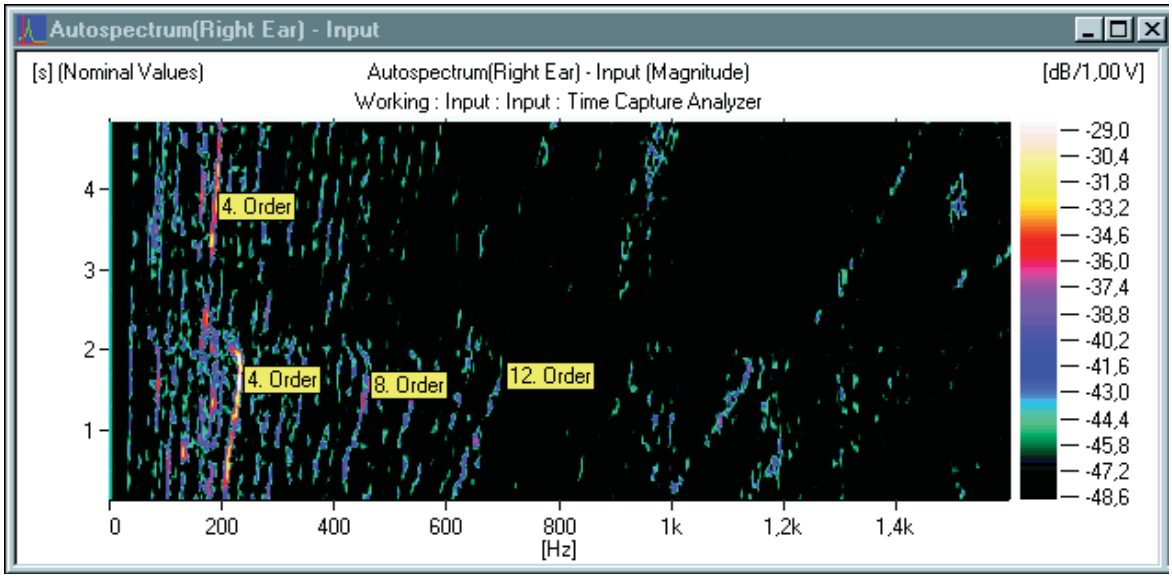

Fig. 43. Contour plot of Sound recording at right ear. Orders 4, 8 and 12, the engine firing harmonics are indicated

For the FFT analysis a 400 Hz baseband, 100 line analysis (T = 250 ms and $\Delta f = 4$ Hz) with Maximum overlap was performed. Maximum overlap was in this case 99,5% since each FFT calculation including averaging etc. took 1,4 ms. Exponential averaging with 1 average was used. Spectra as well as pre-processed order slices were stored into a multi-buffer, using the 1900 RPM of

the drive shaft as a start reference, i.e. used as time zero. Update interval was 10 ms with a total of 551 spectra corresponding to a duration of 5,5 s.

The Time Capture Analyzer was also triggered to start at 1900 RPM making a 5 s recording up to approximately 2800 RPM using a frequency range of 1600 Hz corresponding to a total of 20 480 time samples per channel.

Fig. 43 presents a contour plot of the microphone (time captured) signal from the right ear. 400 lines FFT with 80% overlap and a total of 96 spectra are shown. As expected the contour plot indicates that the dominant frequency content is found along the half-order lines of the engine, especially also at orders 4.0, 8.0 and 12.0, the V-8 engine firing harmonics. As seen the 4th order is the dominating order both before and after the gearshift.

The data represents a typical case of high slew rates, especially the engine RPM at the shift points (up to 2800 RPM/s). Fig. 44 displays the engine RPM curve near the shift from 2nd into 3rd gear, showing the curvefit RPM (smoothed) curve overlaid with the raw estimate (RPM table). The hinge point was found from the raw RPM by using the "display zoom" facility and visual inspection as well as the standard cursor readings, Maximum and Minimum Values (in this case found by PULSE at 1,758 s and at 2,280 s respectively). These numbers were then keyed into the Vold-Kalman RPM Curve Fit property page (see Fig. 13). In the actual calculation the Number of Segments was set to 10 even though fewer segments could have been used successfully.

Fig. 45 shows the magnitude of engine order 4.0, extracted using a three pole Vold-Kalman filter with a relative bandwidth of 20% ($\approx$ 10 Hz). Fig. 46 shows the magnitude of engine order 4.0 using real-time FFT processing. Also an order slice bandwidth of 20% corresponding to approximately 2,5 FFT lines was used for comparison purposes. Due to the record length of 250 ms, all FFT based events are displaced, compared to the Vold-Kalman extracted order, with a delay of 125 ms corresponding to ½ the FFT record length.

When comparing the two 4th order slices the two methods agree extremely well for the slowly changing amplitudes, but the FFT is not able to accurately track the two rapid level changes which are seen in the Vold-Kalman results around the shift point between time 2,0 s and 2,4 s. This is due to the fact that the Vold-Kalman filtering has no slew rate limitations although the real-time FFT was actually able to track the RPM changes in this case. On the other hand the Vold-Kalman filtering provides a better time resolution as well as more data points compared to the FFT technique as explained in the following.

The FFT multi-buffer settings result in 501 data points along the 5 s long Z-axis (25 multibuffer entries per FFT record-length, one entry per 7 FFT calculations). Each FFT record represents approximately 94 ms (= 250 ms $\times$ 37,5%)

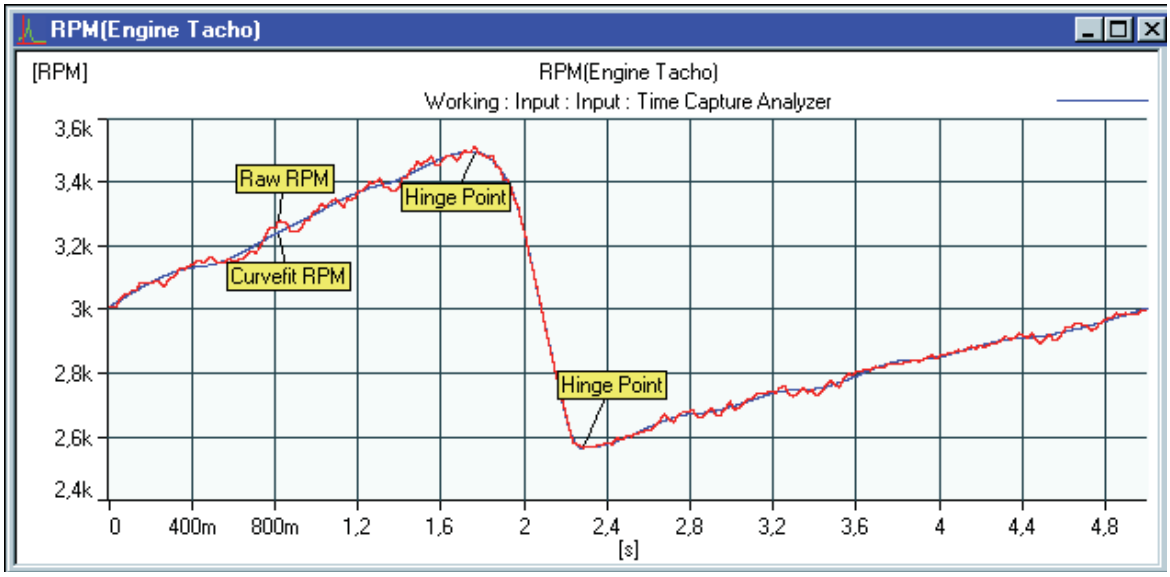

Fig. 44. Detail of the Raw RPM (red colour) and the Curve Fit RPM (blue colour) at the shift point

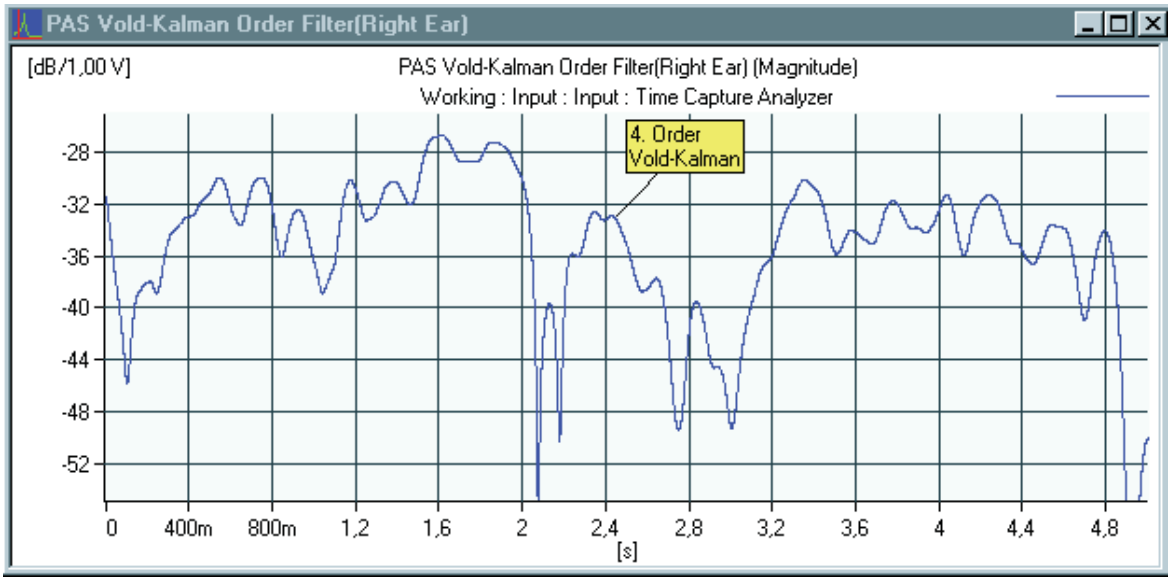

Fig. 45. Engine order 4.0 extracted using Vold-Kalman order tracking filtering. X-axis is displayed from 0 s to 5 s

when using a Hanning weighting function. The effective duration of the Hanning weighting is defined in Ref. [5]. The Vold-Kalman technique results in this case in 20480 data points (as mentioned earlier, for export purposes decimation of the data is possible). The selected frequency bandwidth of 10 Hz corresponds to a length of the IRF of $2\tau = (0{,}2 \times 2 / 10\,\text{Hz}) = 40\,\text{ms}$.

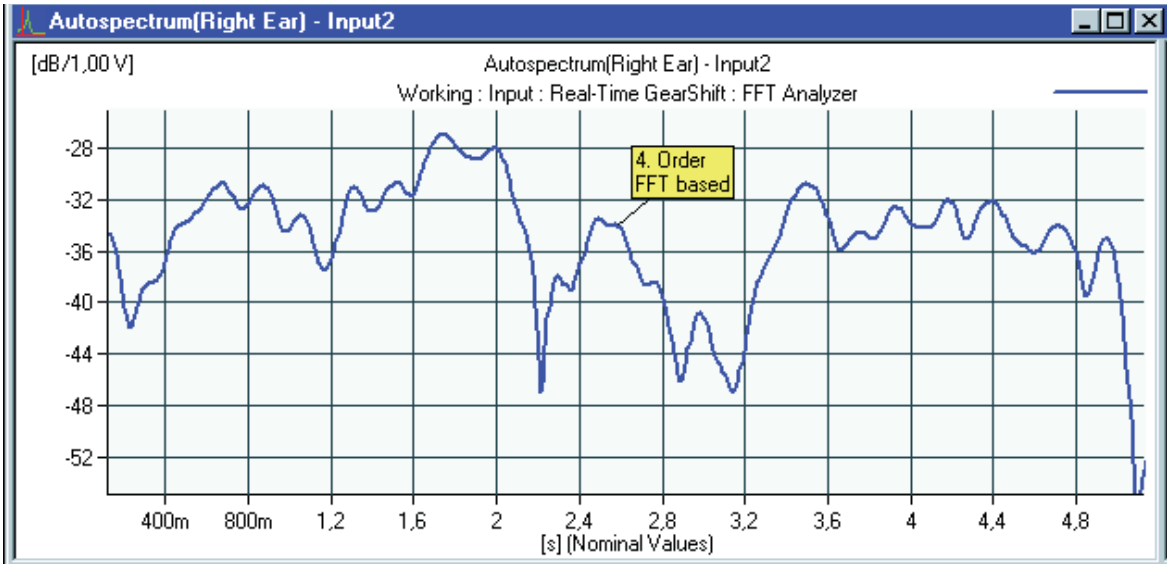

Fig. 46. Engine order 4.0 extracted using real-time FFT processing. X-axis is displayed from 0,125 s to 5,125 s

In order to verify that the 4.0 order was extracted correctly, the order waveform was subtracted from the original signal using the PULSE Sound Quality application. A contour plot of the signal with the 4th order removed was successfully produced using a procedure as described earlier, see Figs. 11 & 40.

In Ref. [3] also a file of the residual sound was generated by extracting the 14 most significant engine orders, and then subtracting this file from the original file. This was done using the MTS* Systems Corporation IDEAS Sound Quality software. The fact that this residual sound has consistently lower levels (about 30 dB) indicates that both the magnitude and phase of the extracted orders were processed with high fidelity, even passing through the gearshift. When listening to the residual sound produced by removing the Vold-Kalman filtered orders, only very little trace of the engine sound was heard through the gearshift. This fact is also a confirmation that the amplitude and phase tracking is very accurate, and it also illustrates the practical value of the Vold-Kalman methods for harmonic extraction and editing in Sound Quality applications involving high slew rates as found at gear shifts.

* Acknowledgement
The tape data was provided by courtesy of MTS Systems Corporation.

Conclusion

The Vold-Kalman filter enables order tracking without tracking-ability slew rate limitations, with only speed limitation due to the filter response time. Phase assigned orders (shown as real, imaginary, magnitude, phase and Nyquist plots) as well as order time waveforms (playback using sound cards) are available. Abrupt changes of the RPM, such as in gear shifts, and tacho drop-outs can be handled and finally decoupling of close and crossing orders is possible. The only disadvantages of the technique is non-real time processing, "longer" calculation time, no information between orders and some prior knowledge of the contents of the signal is required.

The characteristics of the one-pole, two-pole and three-pole Vold-Kalman order tracking filters have been investigated in the time and the frequency domain. The three-pole filter has the best selectivity and therefore the best ability to suppress ripples due to beating interference from the other order components in the signal. In the time response to a tone burst the two- and three-pole filters exhibit small ripples (overshoot). This will, however, only contaminate the results when the signal contains abrupt changes in the amplitude or when the bandwidth of the filter is selected too narrow for the signal.

The time-frequency relationship of the three filter types shows an optimum relationship close to the Heisenberg's uncertainty limit and is given by $B_{3dB} \times \tau = 0.2$, where B_{3dB} is the 3 dB bandwidth of the Vold-Kalman filter and τ is the time it takes for the time response to decay 8.69 dB (a factor of e).

Selection of the bandwidth of the filter should follow $B_{3dB} \geq 2/T_{3dB}$, where T_{3dB} is the time it takes for an order to sweep through the 3 dB bandwidth of a resonance (or the time it takes for an order to change 6 dB in amplitude). In almost all cases the three-pole filter is the best choice due to its better selectivity in the frequency domain. Today the main use of single pole filter is to be able to duplicate processing done in earlier implementation of the Vold-Kalman filtering.

In situations where different orders related to different rotating shafts (tacho signals) are close or crossing each other, decoupling can be used to separate the orders without beating interference.

References

1) Vold, H., Leuridan, J., *"Order Tracking at Extreme Slew Rates, Using Kalman Tracking Filters",* SAE Paper Number 931288, 1993
2) Vold, H., Mains, M., Blough, J., *"Theoretical Foundations for High Performance Order Tracking with the Vold-Kalman Tracking Filter"*, SAE Paper Number 972007, 1997
3) Vold, H., Deel, J., *"Vold-Kalman Order Tracking: New Methods for Vehicle Sound Quality and Drive Train NVH Applications",* SAE Paper Number 972033, 1997
4) Brüel & Kjær, *"PULSE, the Multi-Analyzer System - Type 3560"*, Product Data, BP 1611 - 14, BP 1795
5) Gade, S., Herlufsen, H., Konstantin-Hansen, H., Wismer, N.J., *"Order Tracking Analysis"*, Technical Review No.2, 1995, Brüel & Kjær
6) Blough, J., Brown, D., Vold, H., *"The Time Variant Discrete Fourier Transform as an Order Tracking Method"*, SAE Paper Number 972006, 1997
7) Vold, H., Kundrat, J., Rocklin, G., Russell, R., *"A Multi-Input Modal Estimation Method for Mini-Computers"*, SAE Paper Number 820194, 1982
8) Kalman, R. E., *"A new approach to linear filtering and prediction problems"*, Trans. Amer. Soc. Mech. Eng., J. Basic Engineering, 82, 32–45, 1960
9) Kalman, R. E., Bucy, R. S., *"New results in linear filtering and prediction theory"*, Trans. Amer. Soc. Mech. Eng., J. Basic Engineering, 83, 95–108, 1961
10) Vold, Herlufsen, Mains, Corwin-Renner, *"Multiple Axle Order Tracking with the Vold-Kalman Tracking Filter"*, Sound and Vibration Magazine, 30–34, May 1997
11) Leuridan, J., Van der Auweraer, H., Vold, H., *"The Analysis of Nonstationary Dynamic Signals"*, Sound & Vibration Magazine, 14–26, August 1994
12) Randall, R.B., *"Frequency Analysis"*, Brüel & Kjær, 1987
13) Brigham, E.O., *"The Fast Fourier Transform"*, Prentice-Hall, Inc.,Englewood Cliffs, N.J., 1974
14) Gade S., Herlufsen. H., Konstantin-Hansen, H., Ladegaard, P., *"Simultaneous Zwicker Loudness and One Third Octave Measurements"*, Internoise Proceedings, Christchurch, NZ, 1998
15) Gade S., Herlufsen. H., *"Use of weighting Functions in DFT/FFT Analysis"*, Brüel & Kjær Technical Reviews Nos. 3 & 4, 1987

16) Brüel & Kjær, *"Vold-Kalman Order Tracking Filter – Type 7703"*, Product Data, BP 1760
17) Brüel & Kjær, *"Time Capture – Type 7705"*, Product Data, BP 1762
18) Brüel & Kjær, *"Order Analysis – Type 7702"*, Product Data, BP 1634
19) Gade S., Herlufsen. H., *"Digital Filter Techniques vs. FFT Techniques for Damping Measurement"*, Brüel & Kjær Technical Review No. 1, 1994
20) Leuridan, J., Kopp, G.E., Moshrefi, N., Vold, H., *"High Resolution Order Tracking Using Kalman Tracking Filters – Theory and Applications"*, SAE Paper Number 951332, 1995
21) Gade, S., Gram-Hansen, K., *"Non-stationary Signal Analysis using Wavelet Transform, Short-time Fourier Transform and Wigner-Ville Distribution"*, Brüel & Kjær Technical Review Nos. 2, 1996

Appendix A

We have observed that all time response curves are crossing at –6 dB at the two points in time where the applied tone burst is started and where it is discontinued, Figs. 21 & 22. At theses points in time we have that ½ the filter time response contains the signal while the rest of the filter time response contains no signal. Thus the overall time response has decayed by 3 dB (half power) while the signal inside the tracking filter has decayed by 6 dB. A similar phenomena is observed using FFT analysis and is explained in details in the following.

As an illustration, an FFT analysis using 400 lines, frequency range of f_{span} = 1600 Hz, resolution of Δf = 4 Hz and a record length of 250 ms is used. A sinusoidal signal of $1V_{rms}$, 800 Hz (i.e., 200 periods) is analyzed as shown in Fig. A1. Cursor readings show in Fig. A2 the level to be 0 dB at 800 Hz as well as the total power is 0 dB. No leakage is seen.

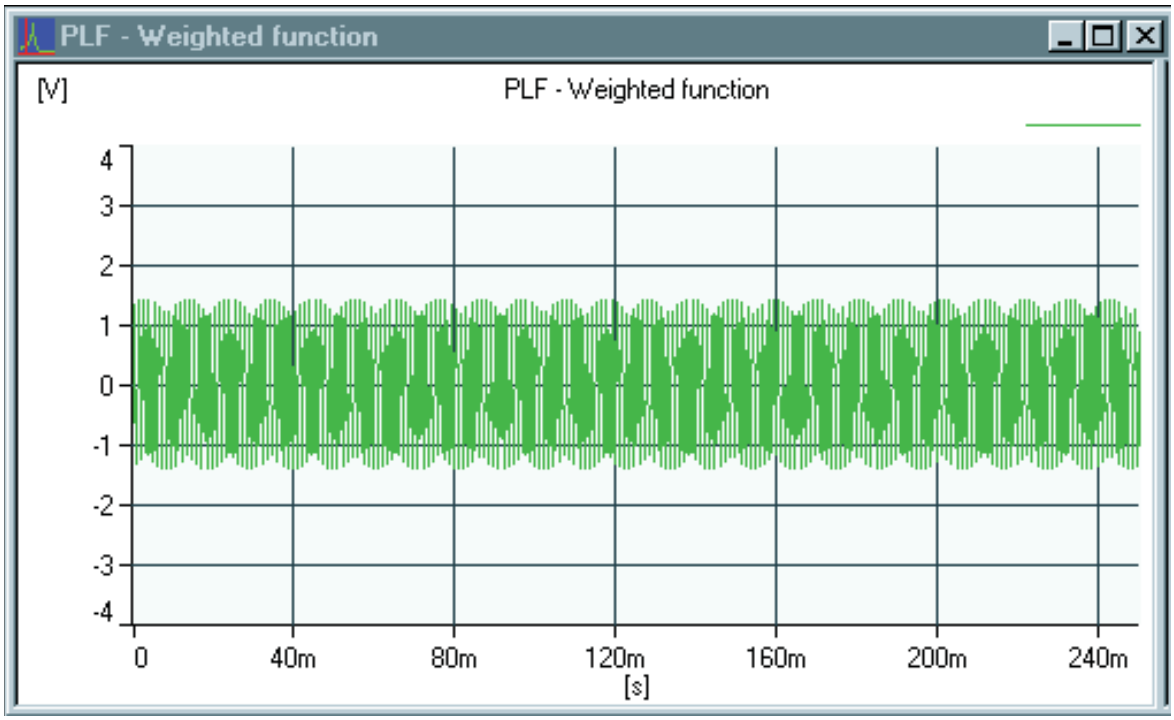

Fig. A1. Time signal of a $1V_{rms}$, 200 period, 800 Hz sine wave analyzed using a rectangular weighting function

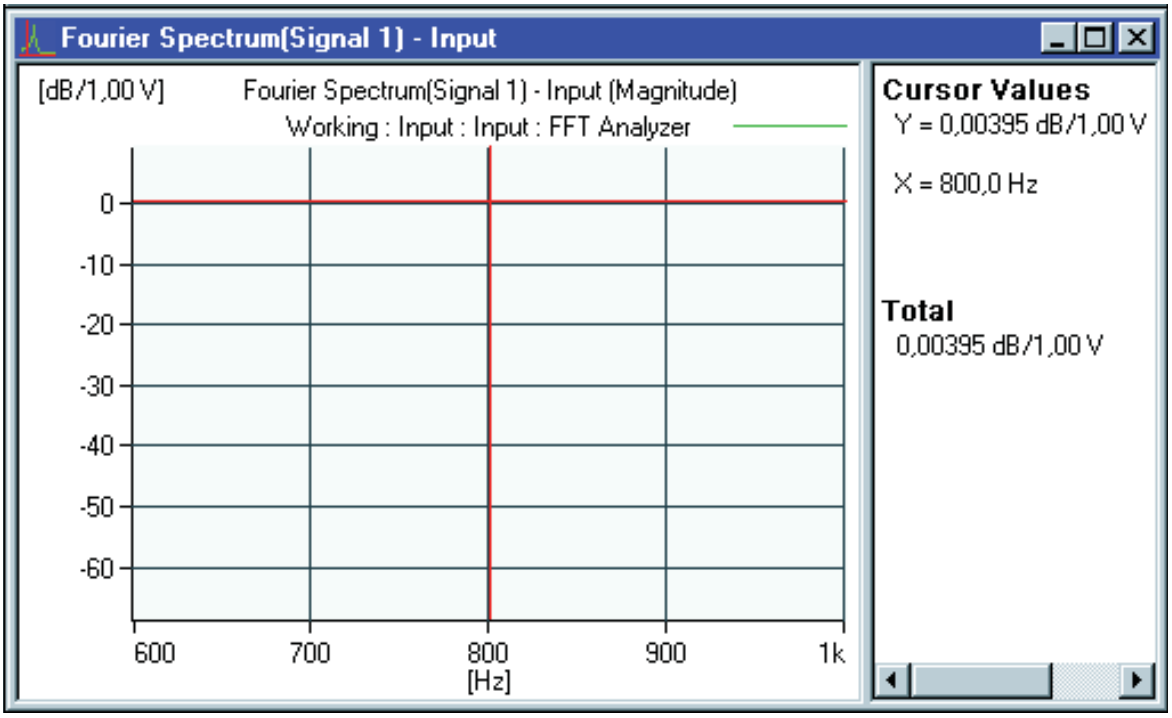

Fig. A2. Frequency spectrum of a 200 period, 800 Hz sine wave analyzed using a rectangular weighting function, no leakage is seen

Using a rectangular weighting with an amplitude of A and time length of T results in a spectrum weighting of

$$H(f) = AT \times \sin(\pi Tf) / (\pi f) \tag{A1}$$

which is convolved with the spectrum of the 800 Hz signal and then sampled (in this case) at frequencies which is multiples of $\Delta f = 4$ Hz. The weighting function and its corresponding spectrum are shown in Fig. A3. A main lobe with a maximum amplitude of AT and a width of $2\Delta f$ is shown, and all side lobes have a width of Δf. In this case the spectrum is sampled at the centre of the main lobe and at all zero crossings between the lobes resulting in a calculated/displayed FFT spectrum consisting of one line only, which is scaled to an amplitude value of 1 corresponding to 0 dB. See Ref. 12 (Appendix A) and Ref. 13 (Chapter 2).

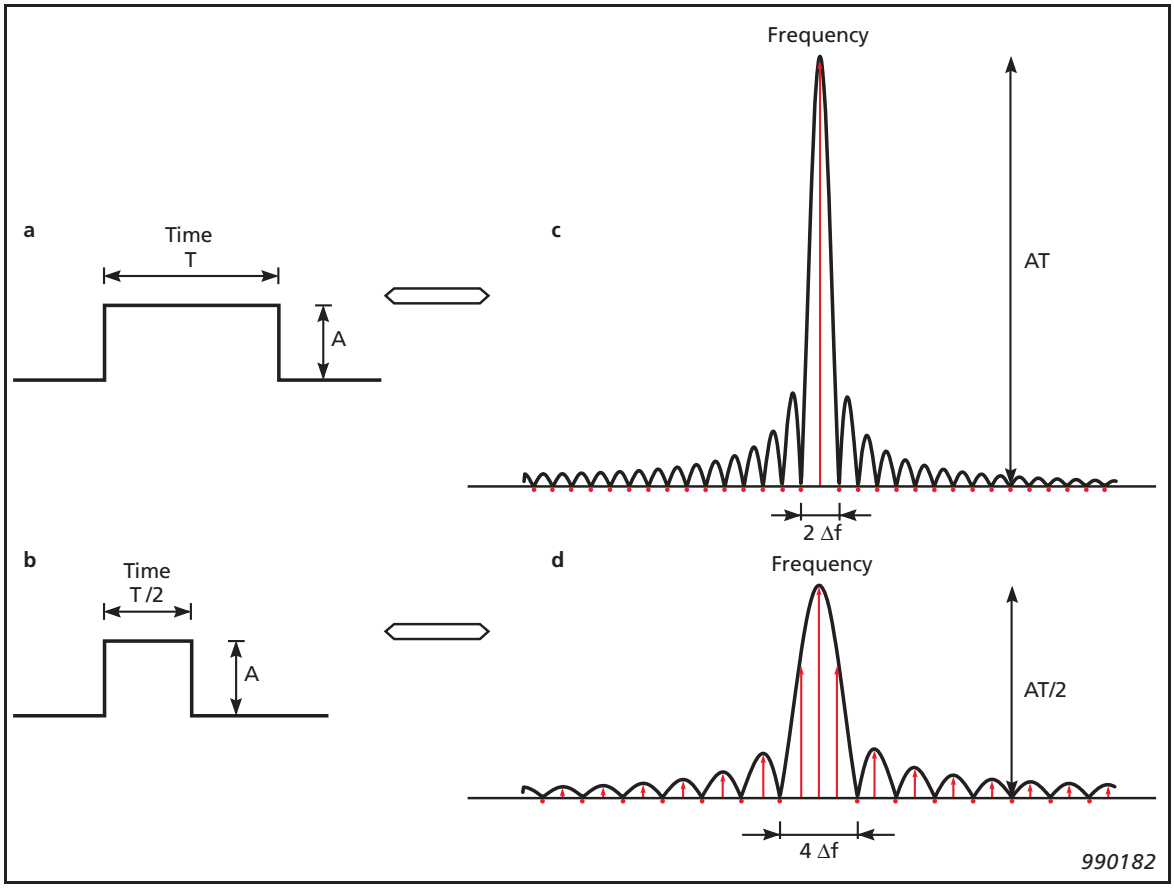

Fig. A3. Time and frequency scaling of a rectangular weighting function

Now the second half of the record is zero padded, corresponding to using a rectangular weighting function with same amplitude, A, but of half the length, T/2. See Fig. A4. This weighting results in a spectrum

$$H(f) = AT/2 \times \sin(\pi Tf/2) / (\pi f) \qquad \text{(A2)}$$

which is shown in Fig. A3. All the lobes have double width compared to the non-zero padded case, i.e. the main lobe has a width of 4Δf and the side lobes have a width of 2Δf. The amplitude has decreased by a factor of 2, corresponding to −6dB. Thus the corresponding FFT spectrum of the 800 Hz sine wave will show a line spectrum where the main lobe is sampled 3 times and furthermore sampled at the centre of all side lobes as well as at the zero crossings between all lobes. See Fig. A5. The amplitudes/levels of the individual FFT lines follow the well known sequence, 1, 2/π, 2/3π, 2/5π, 2/7π, … , see Fig. 2.15 in Ref. [12].

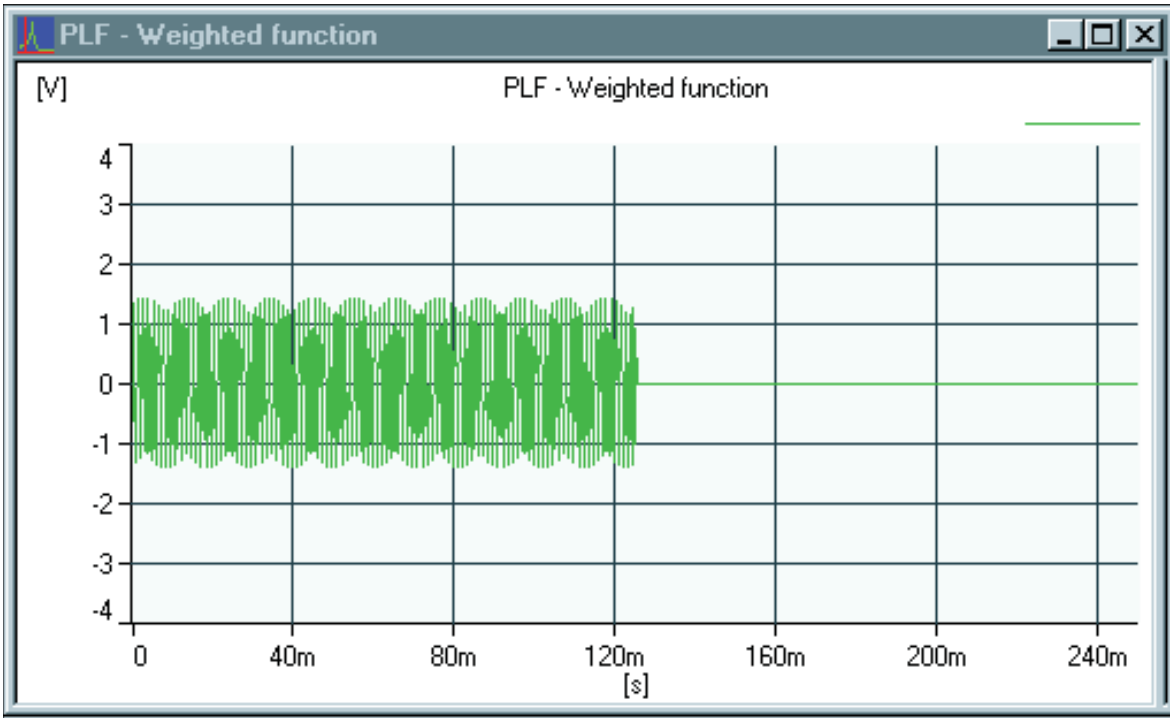

Fig. A4. Time signal of a 200 period, 800 Hz sine wave analyzed using half a rectangular weighting function, i.e. only 100 periods are within the window

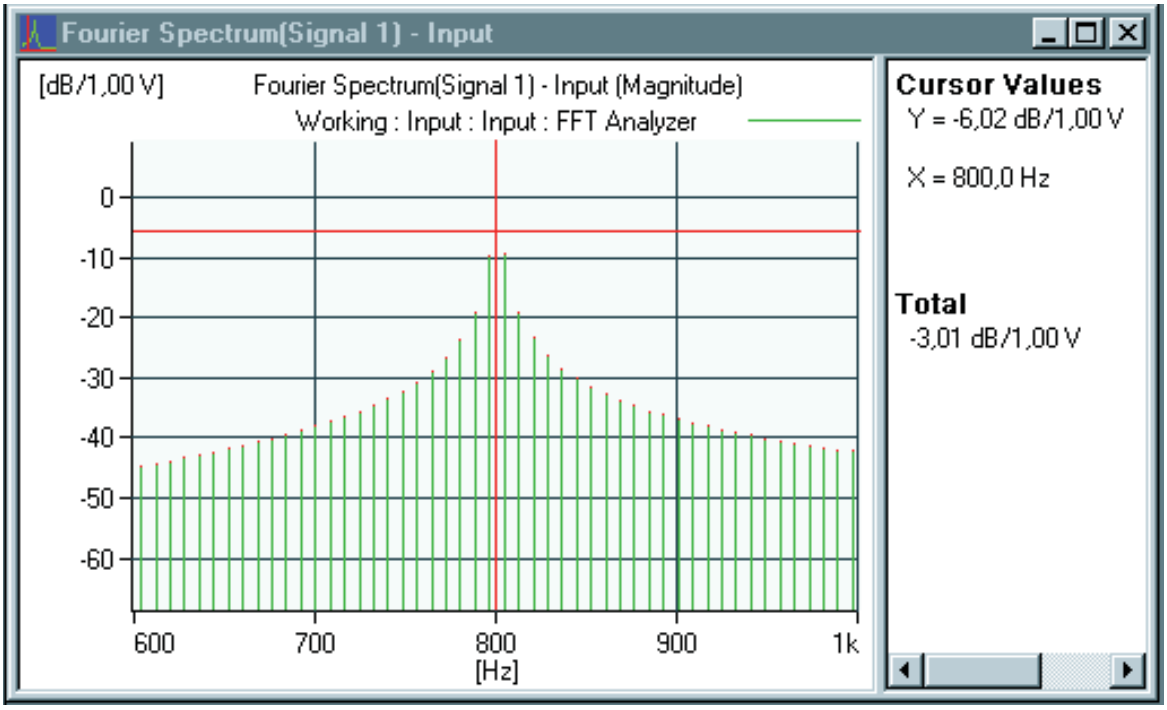

Fig. A5. Frequency spectrum of a 200 period, 800 Hz sine wave analyzed using half a rectangular weighting function, i.e. only 100 periods are within the window

The cursor readings show a level of –6 dB at 800 Hz as expected according to the discussion above. The total level is –3 dB (half power), which is also expected since the time window contains data in only half the record in this case.

This is also the case using other time weighting functions as long as they are symmetrical in time. Figs. A6 & A7 show the results using Hanning weighting.

In this case the resulting spectrum is most easily understood by convolving the FFT spectrum shown in Fig. A5, with the FFT spectrum of a Hanning weighting function, taking amplitude as well as phase into account. The phase of the spectrum shown in Fig. A5 is +90 degrees for all non-zero amplitude values at frequencies lower than the centre frequency, 0 degrees at the centre frequency and –90 degrees for all non-zero amplitude values at frequencies higher than the centre frequency, see Fig. 2.24 Ref. [12]. The Fourier spectrum of a Hanning (scaled to an amplitude of 2 in the centre of the record) consists of three values, 1 at the centre frequency, f_0 and –½ (or ½ and a phase of 180°) at the two neighbouring frequencies, $f_0 - \Delta f$ and $f_0 + \Delta f$. From the mean square values the Noise Bandwidth of the Hanning weighting is found to be $1^2 + ½^2 + ½^2 = 1.5$ or 1.76 dB. See ref. [15].

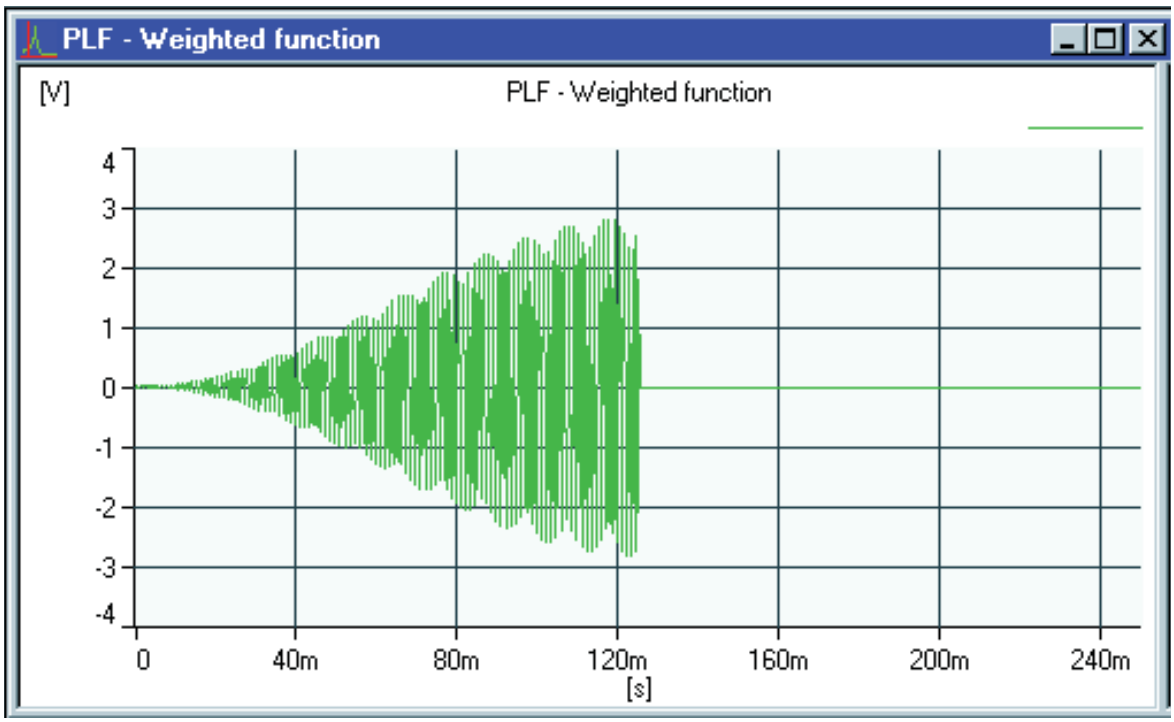

Fig. A6. Time signal of a 200 period, 800 Hz sine wave analyzed using half a Hanning weighting function, i.e. only 100 periods are within the window

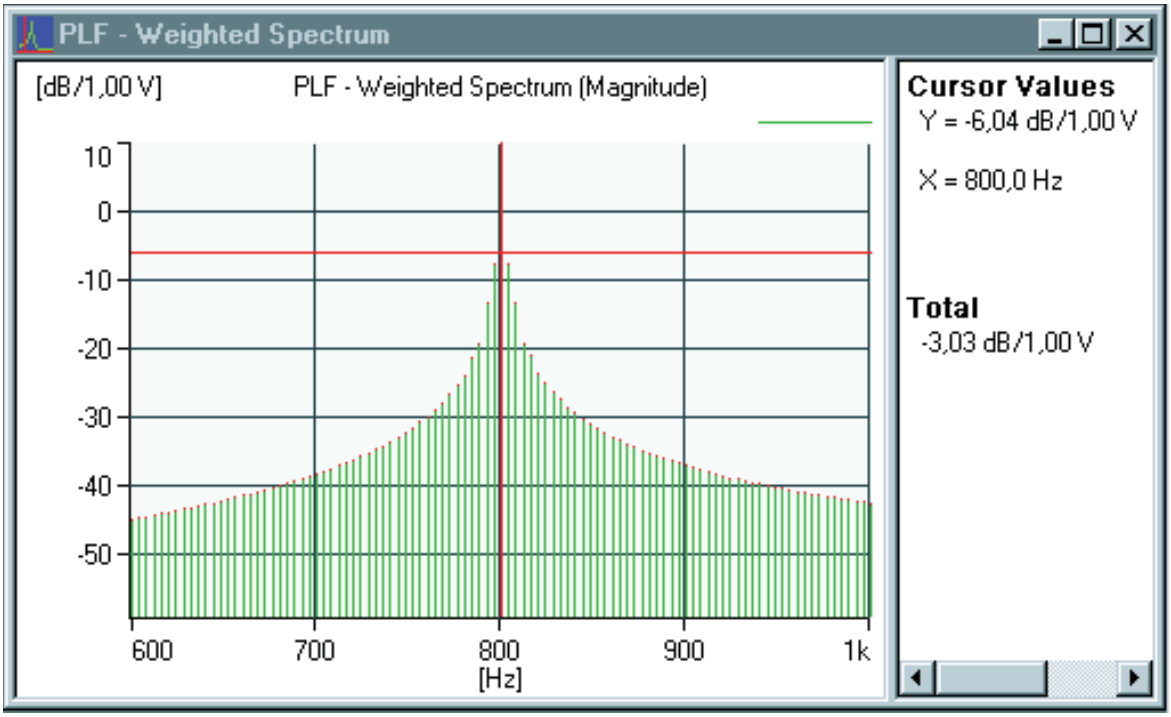

Fig. A7. Frequency spectrum of a 200 period, 800 Hz sine wave analyzed using half a Hanning weighting function, i.e. only 100 periods are within the window

Convolution of the spectrum in Fig. A5 with the spectrum of a Hanning results in the spectrum shown in Fig. A7 as explained in the following.

When one of the zero values are convolved with the Hanning the result is an amplitude value which is the mean value of the two adjacent lines but with opposite phase.

When one of the non-zero side lobe values are convolved with the spectrum of a Hanning, the original value is unchanged due to the fact that the two adjacent lines have zero amplitude values.

When the centre frequency value at f_0 is convolved with the spectrum of a Hanning the original is unchanged due to the fact that the two adjacent lines have equal amplitude but opposite phase.

To convolve the two lines adjacent to the centre frequency with the spectrum of the Hanning requires a little more complex calculation, resulting in a slight increase in amplitude from 0.32 (–9.9 dB) to 0.40 (–7.9 dB) and a phase change from respectively 90° to 128° for the left, $(f_0 - \Delta f)$ and –90° to –128° for the right, $(f_0 - \Delta f)$ FFT line.

Thus for the resulting spectrum shown in Fig. A7 the centre line will also in this case show a level of –6 dB and the total power of the spectrum –3 dB, after

compensating the total reading for the Noise Bandwidth (1.76 dB) of the Hanning weighting.

Conclusion

When the FFT time record contains a stationary sinusoidal signal in only the first or the last half of the record the total power of the spectrum is decreased by 3 dB irrespective of choice of weighting function as long as this function is symmetrical in the record. Half of the power/energy of this signal (–6 dB) is found at the expected frequency while the rest (–6 dB) is found as leakage. Using a Vold-Kalman order tracking filter, which also has a symmetrical time response, the leakage components are normally not seen, while the –6 dB level of the tracking frequency is observed in the time response as discussed above as well as shown in Fig. 22.

Previously issued numbers of Brüel & Kjær Technical Review

(Continued from cover page 2)

4 – 1986 Field Measurements of Sound Insulation with a Battery-Operated Intensity Analyzer
Pressure Microphones for Intensity Measurements with Significantly Improved Phase Properties
Measurement of Acoustical Distance between Intensity Probe Microphones
Wind and Turbulence Noise of Turbulence Screen, Nose Cone and Sound Intensity Probe with Wind Screen

3 – 1986 A Method of Determining the Modal Frequencies of Structures with Coupled Modes
Improvement to Monoreference Modal Data by Adding an Oblique Degree of Freedom for the Reference

2 – 1986 Quality in Spectral Match of Photometric Transducers
Guide to Lighting of Urban Areas

1 – 1986 Environmental Noise Measurements

4 – 1985 Validity of Intensity Measurements in Partially Diffuse Sound Field
Influence of Tripods and Microphone Clips on the Frequency Response of Microphones

3 – 1985 The Modulation Transfer Function in Room Acoustics
RASTI: A Tool for Evaluating Auditoria

2 – 1985 Heat Stress
A New Thermal Anemometer Probe for Indoor Air Velocity Measurements

1 – 1985 Local Thermal Discomfort

Special technical literature

Brüel & Kjær publishes a variety of technical literature which can be obtained from your local Brüel & Kjær representative.
The following literature is presently available:

- Acoustic Noise Measurements (English), 5th. Edition
- Noise Control (English, French)
- Frequency Analysis (English), 3rd. Edition
- Catalogues (several languages)
- Product Data Sheets (English, German, French,)

Furthermore, back copies of the Technical Review can be supplied as shown in the list above. Older issues may be obtained provided they are still in stock.

BV 0052 – 11 ISSN 0007–2621

HEADQUARTERS: DK-2850 Nærum · Denmark
Telephone: +45 45 80 05 00 · Fax: +45 45 80 14 05
Internet: http://www.bk.dk · e-mail: info@bk.dk

Brüel & Kjær